Structural controls on the Triassic Main Buntsandstein sediment distribution in the Roer Valley Graben, the Netherlands

Emilio Cecchetti[1] , Allard W. Martinius[1,2], Pierre-Olivier Bruna[1] ,
Annelies Bender[3] and Hemmo A. Abels[1]

[1]Faculty of Geoscience and Engineering, Delft University of Technology, Delft, The Netherlands; [2]Equinor ASA, Trondheim, Norway and [3]Aardyn B.V., Dordrecht, The Netherlands

Abstract

The lower Triassic Main Buntsandstein Subgroup represents a promising, but high-risk geothermal play in the Netherlands. Although the gross thickness in boreholes locally exceeds 200 m, the spatial distribution, geometries and preservation of these sedimentary units remained uncertain due to the lack of seismic data with sufficient resolution and the sparse borehole network. This creates uncertainty in the quantification of the aquifer dimensions that is essential for the planning of geothermal operations.

In this study, seismic interpretation and 2D palinspastic restoration of new and reprocessed seismic data were conducted and combined with borehole data to assess the tectonic evolution of the Roer Valley Graben in the southeastern Netherlands and its control on the spatial distribution of the Main Buntsandstein Subgroup sediments. Our results show that the central and southern parts of the Roer Valley Graben were active depocenters in the Early to Middle Triassic times dominated by fluvial sandstone deposition, providing important play elements for prospective leads on geothermal exploration. The northern part of the basin was a more marginal area where mostly fine-grained sediments were deposited. To the northwest, differential subsidence resulted in the development of areas where the Buntsandstein thickness is reduced to ~150 m.

After deposition, the Main Buntsandstein sediments were compartmentalised by faulting related to post-depositional tectonic activity, locally reducing the lateral extent of the geothermal target areas down to 1–2 km in a ~NE–SW direction. On the platform areas adjacent to the Roer Valley Graben and to the southeast, Jurassic sediments are largely absent and the Main Buntsandstein sediments are present at depths shallower than 2 km. These platforms are promising targets for further investigation, as the relatively shallow burial depths, compared to the central part of the Graben, may have contributed to the preservation of more favourable reservoir properties.

Introduction

The lower Triassic Main Buntsandstein Subgroup is considered to be a promising geothermal play in the subsurface of the Netherlands (Kramers et al., 2012; Mijnlieff, 2020). In the Roer Valley Graben in the southeastern Netherlands, the Main Buntsandstein Subgroup is composed of stacked sandstones locally reaching total thicknesses of over 200 m and temperatures of 80–130°C at depths of 2–4 km (IF Technology, 2012; Kramers et al., 2012; Mijnlieff, 2020). This makes the Main Buntsandstein sediments an attractive deep geothermal play that could contribute to open-up the geothermal potential in an area where geothermal energy is rather underdeveloped (Ministry of Economic Affairs and Climate Policy, 2023).

The Roer Valley Graben area is a geologically under-explored area compared to the adjacent West Netherlands Basin or the offshore sector (Van Lochem et al., 2019). It is mostly covered by 2D seismic surveys of different ages and qualities, with a series of wells penetrating the lower Triassic Main Buntsandstein Subgroup in focused, tectonically high areas. The limited character of the geological dataset increases uncertainties for geothermal operations in an area where several tectonic phases resulted in a network of faults with different orientations and characters, creating complex geometries and architectures during and after deposition (Geluk et al., 1994; Deckers et al., 2023). These complexities can affect the Buntsandstein thickness, lateral extent and properties, which are key parameters controlling the level of injectivity and lifetime of a geothermal system (Willems et al., 2020).

In this study, we evaluate the impact of the structural evolution on the distribution, character and preservation of the Main Buntsandstein sediments in the Roer Valley Graben. The sediment depth and thickness variations are outlined by seismic mapping, as are the visible faults. These parameters, combined with well data, are essential to determine the extent, lithology and

geometry of the Main Buntsandstein sedimentary units. Then, 2D restoration analysis is performed on a network of transects up to the base of the Main Buntsandstein to assess the structural evolution of the basin, the burial history of the lower Triassic sediments and reconstruct the basin geometry at the time of deposition of the Main Buntsandstein units. Finally, the results of this evaluation and its intrinsic uncertainties are discussed, and recommendations for future geothermal exploration in the southeastern part of the Netherlands are proposed.

Regional geological setting

The Roer Valley Graben

The subsurface in the southeastern part of the Netherlands is characterised by the presence of several structural elements, with the Roer Valley Graben being the most prominent (Fig. 1). The Roer Valley Graben is a NW-SE oriented Graben forming the propagation of the most western branch of the Rhine Graben rift system, a Cenozoic rift system that extends from the Alps to the North Sea area (Ziegler, 1992).

In its present-day form, the Roer Valley Graben is ~20–45 km wide and 130 km long, bounded to its NE flank by the Peel-Maasbommel Complex (Fig. 1). To the southwest, the Oosterhout Platform and the Zeeland High separate the Roer Valley Graben from the Campine Basin and the London Brabant Massif further to the south (Kombrink et al., 2012; Deckers et al., 2023). To the northwest, the Roer Valley Graben continues into the West Netherlands Basin, where the fault direction changes from overall NW–SE to more WNW–ESE striking (Geluk et al., 1994; NITG, 2004; Worum et al., 2005).

Structural evolution

The structural evolution of the study area began during the Caledonian Orogeny in the Devonian, when the London-Brabant Massif was uplifted and the Campine basin formed a large depression to the north (Geluk et al., 1994; NITG, 2004). However, it was only during Late Carboniferous times that as a result of the Variscan Orogeny the precursor structure of the Roer Valley Graben and Peel-Maasbommel Complex started developing (NITG, 2004).

During Late Permian to Late Triassic times, a regime of extensional tectonics led to basin subsidence, allowing the accommodation of a thick sequence of sediments in the Roer Valley Graben area (Zijerveld et al., 1992; Geluk, 2005; NITG, 2004). The Roer Valley Graben formed a ~NW–SE oriented half-Graben developed as result of fault activity along the northern margin of the London-Brabant Massif (Winstanley, 1993; Geluk, 2005). To the north of the Roer Valley Graben, the Central Netherlands Swell was a positive topographic element where only minor sedimentation occurred (Geluk and Röhling, 1997).

From the Late Jurassic to the Early Cretaceous, the Mid- and Late-Kimmerian tectonic phases marked a further structural reorganisation. The Mid-Kimmerian tectonic phase led to the uplift of block terrains adjacent to the Roer Valley Graben, such as the Peel Complex and the Zeeland High. Then, differential fault movements during the Late-Kimmerian resulted in further uplift of the block terrains and the development of sub-Graben systems within the Roer Valley Graben. These tectonic phases locally caused deep truncation and erosion of Mesozoic deposits across the Roer Valley Graben area (Winstanley, 1993; Geluk et al., 1994; NITG, 2004; Kombrink et al., 2012).

During the Middle to Late Cretaceous, regional subsidence accompanied by sea-level rise resulted in the deposition of the Chalk Group (Herngreen and Wong, 2007). The deposition of the Chalk Group on top of older sediments of Early Cretaceous (Berriasian) to Carboniferous age resulted in the development of an unconformity, which is referred to in this article as the base Chalk Group unconformity.

After the deposition of the Chalk Group, the Roer Valley Graben was inverted as result of the convergence between Africa and Europe (De Jager, 2003). This caused deep erosion in the Graben area, while the flanks continued to subside (Winstanley, 1993). The Roer Valley Graben was then reactivated as part of the Rhine Graben rift system during the Late Oligocene (Geluk et al., 1994; Deckers et al., 2023).
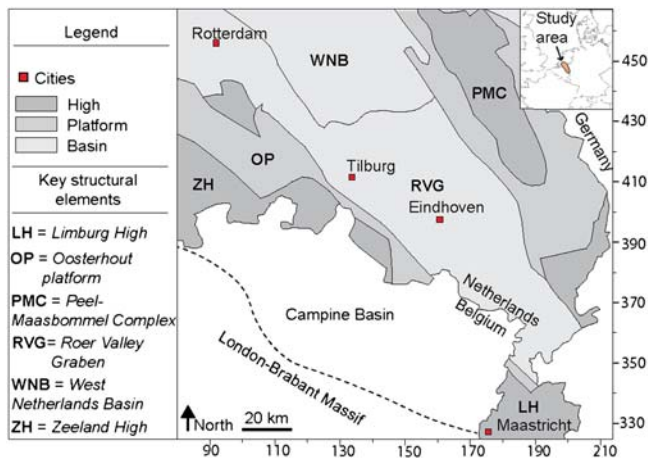
The main Buntsandstein subgroup

During the Early to Middle Triassic, the Roer Valley Graben was part of the Germanic Basin, a large endorheic basin located at the western margin of the Tethys domain (Geluk, 2005; Bachmann et al., 2010; Bourquin et al., 2011). The Germanic Basin extended from England in the west to the eastern border of Poland in the east, resulting in the widespread sedimentation of the Main Buntsandstein sediments across northern Europe (Geluk, 2005).

In the Dutch lithostratigraphic nomenclature, the Main Buntsandstein Subgroup is subdivided into three formations: the Volpriehausen, Detfurth and Hardegsen Formations (Van Adrichem Boogaert and Kouwe, 1993). The Volpriehausen and Detfurth Formations represent each a sequence of sediments in which a basal fluvial/aeolian sandstone unit is overlain by a playa-lake claystone unit (Geluk and Röhling, 1997). In the Roer Valley Graben, these playa-lake claystone units are largely absent, and locally substituted by their time-equivalent basin-fringe sandstones (Van Adrichem Boogaert and Kouwe, 1993; Kortekaas et al., 2018). The Hardegsen Formation is instead characterised by an alternation of fluvial sandstone and claystone at the meter to tens-of-metre scales (Fig. 1b) (Van Adrichem Boogaert and Kouwe, 1993; Geluk and Röhling, 1997).

Across northern European basins, the top of the Main Buntsandstein is often associated with the Hardegsen unconformity that locally truncates and erodes the lower Triassic sediments (Linol et al., 2009; Pharaoh et al., 2010; Bourquin et al., 2011). However, this unconformity has not been observed in the Roer Valley Graben, where the Main Buntsandstein stratigraphy is reported to be entirely preserved (Geluk, 2005).

In the Roer Valley Graben, the sedimentation of the Main Buntsandstein Subgroup occurred through fluvial systems grading northwards into playa-lake deposits (Geluk, 2005). Sediments were supplied by source terrains over distances of 50–150 km from adjacent basin flanks (Mckie and Willems, 2009) and via major river systems over 200–400 km from remote catchment areas, which suggests substantial precipitation in the distant catchments (Audley-Charles, 1970; Mckie and Willems, 2009). Based on heavy mineral analysis, the London Brabant Massif located to the southwest represents an important source for the Main Buntsandstein sediments during the Early to Middle Triassic in the Germanic Basin (Olivarius et al., 2017). In parallel, the Armorican Massif in northeastern France and the Rhenish Massif

Figure 1. Main structural elements at present-day in the southern part of the Netherlands (after Kombrink et al., 2012). The Main Buntsandstein sediments are present in the basin and the platforms, while they are not encountered in the highs.

in northwestern Germany are considered more distant sediment sources (Bourquin et al., 2009; Bachmann et al., 2010).

Data and Methods

The dataset

To conduct this study, thirty-five 2D seismic profiles, two 3D seismic surveys (L3CLY1992A_1 and L3NAM1988A-2), and data from 33 wells have been collected and analysed (Fig. 2). In addition, other 2D vintage seismic profiles have been consulted when interpretation was uncertain or lateral variability needed to be assessed beyond the study area. 2D seismic lines make up a regional grid of the study area, while the 3D seismic volumes provide additional data in the area around Tilburg. Most of the data can be publicly downloaded through NLOG (www.nlog.nl), including the eleven regional 2D seismic lines acquired within the framework of the SCAN project (www.scanaardwarmte.nl). Eighteen reprocessed and six recently acquired 2D seismic lines have been made available for the study by Aardyn B.V.

The seismic dataset was acquired through several campaigns by different operators, thus corrections in datum and seismic polarity convention were applied. Well data include gamma-ray, density and sonic logs, checkshot data, mudlogs, cuttings and core photos, which were mainly used to: i) determine the seismic response of the different horizons at well scale; ii) calculate time-to-depth relationships and iii) analyse lithologies. The well dataset also includes 3 wells from the Belgian side of the Roer Valley Graben (courtesy of VITO). The regional velocity model 'VELMOD-2' was employed to convert the interpretations from time to depth domain. Input parameters for the VELMOD-2 include velocity data from the main lithostratigraphic units in the subsurface of the Netherlands. For more information on the velocity model see https://www.nlog.nl/en/velmod-2.

Wireline interpretation

Wireline logs were used to mark the boundary between the major lithological units present in the subsurface, allowing the identification of the principal horizons of interest for the study such as the top and the base of the Main Buntsandstein. First, the true stratigraphic thickness was determined at borehole scale by

integrating well path surveys and structural dip obtained through seismic interpretation. To assess lithological changes within the Main Buntsandstein sequence, a gamma-ray cut-off was applied to separate shales from sands. The cut-off was chosen according to the grain sizes extracted through the analysis of core material from different wells in the study area (Fig. 2). By plotting the gamma-ray distribution of the cored interval, a clear bimodal distribution revealed the most appropriate value for the cut-off being 90 American Petroleum Institute (API) (Fig. S1 in Appendix). The cut-off application produces the first net sand thickness at well scale. The net sand thickness value was subsequently divided by the true stratigraphic gross thickness to estimate an average N/G ratio for the stratigraphic interval.

Seismic interpretation

The seismic interpretation was carried out in the Petrel software (www.software.slb.com). The Society of Exploration Geophysicists (SEG) seismic polarity convention (Veeken and van Moerkerken, 2013) was adopted to harmonise seismic input data, and a mis-tie analysis between seismic datasets was performed by applying a constant correction through cross-cutting seismic lines without changing the initial structure of the seismic data. Misfits were resolved manually by matching the Triassic reflectors at the expense of the shallower counterparts. Checkshot data were used where available to calibrate the sonic log and increase the accuracy in the seismic-to-well tie process. As part of the seismic-to-well tie, a synthetic seismogram was calculated to tie the horizons of interest to the seismic reflectors (Fig. 3).

Seismic interpretation was conducted by mapping horizons and faults to reveal the main stratigraphic architecture of the study area and the controls on the Main Buntsandstein depth and thickness. Horizons were interpreted based on ties with borehole data (Fig. 3). Once horizons were picked on the seismic line along the boreholes, the interpretation was extended to surrounding seismic lines. Fault timing was investigated based on the identification of syn-sedimentary sequences, and the main deformation phases in the study area were reconstructed. Faults interpreted in multiple 2D lines and considered part of the same fault plane were grouped together in the same fault set and used for the computation of the geological maps. Fault planes and lithostratigraphic horizons from the digital geological model (DGM) were locally used as proxy to laterally extend the faults and horizons interpreted within this study. The DGM data are publicly available and can be downloaded from www.nlog.nl. The horizons mapped as the top and the base of the Main Buntsandstein were then used to build structural depth maps deploying Petrel's convergent interpolation algorithm. This algorithm estimates values at locations within the data point neighbourhood based on the known values at the data points until convergence is reached. These maps were subsequently used as a trend map in combination with well data to construct maps of the Main Buntsandstein total thickness, sandstone thickness and N/G.

The geological complexity of the subsurface and the presence of strong reflectors like those associated with the Posidonia Shale and the Chalk Group overlying the lower Triassic sediments locally absorb, backscatter and reduce the amount of energy transmitted to deeper layers. Thus, a study of the reflection geometries, such as the amplitude, configuration, continuity and terminations of the Main Buntsandstein reflectors, was conducted near well locations by extrapolating information of the rock units from the wellbore. This was done
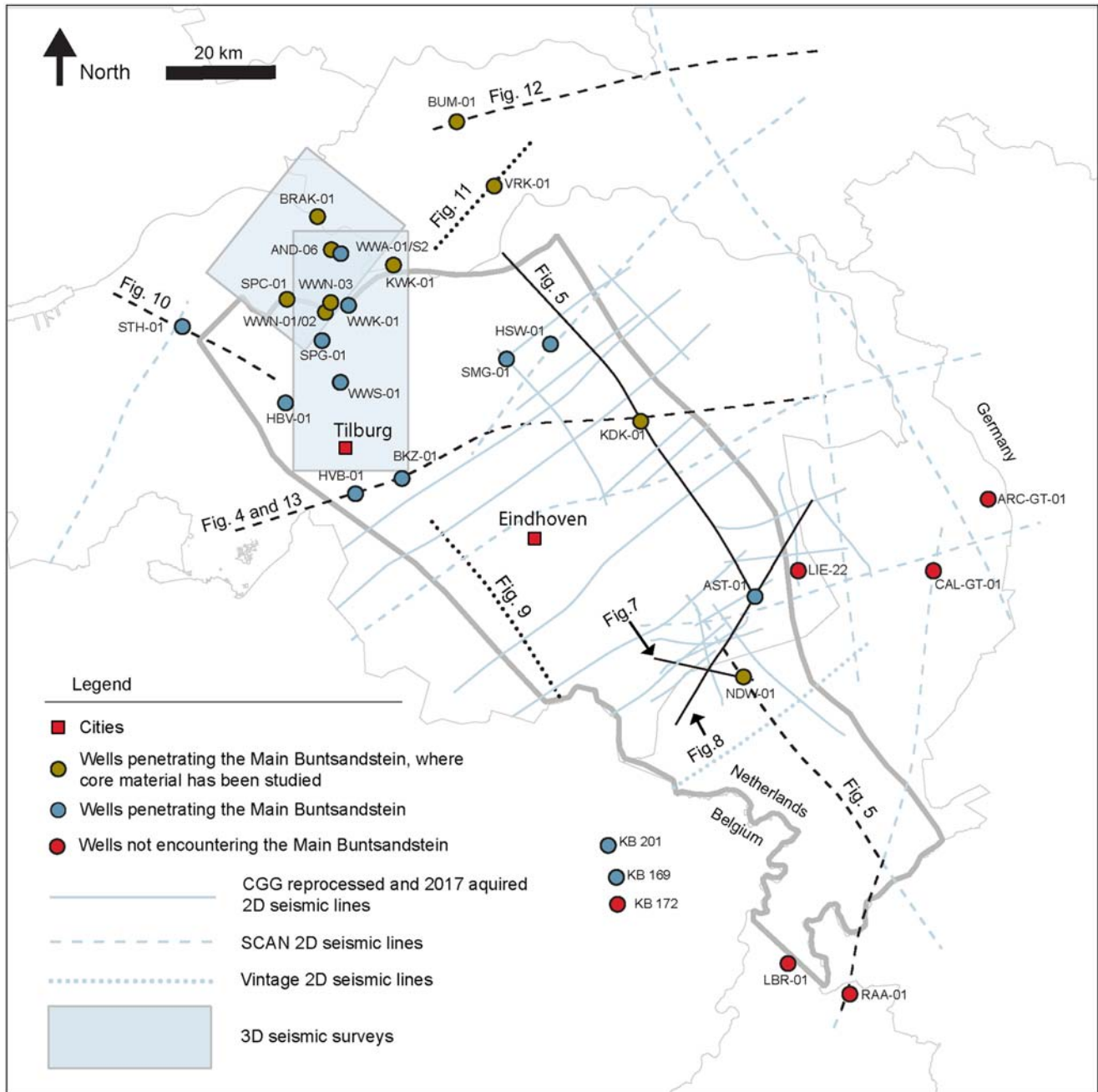
Figure 2. Overview of the data used for this study. The 2D seismic transects displayed are composed by SCAN lines, CGG reprocessed and 2D lines acquired in 2017. The lines in black correspond to the seismic lines interpreted and shown in this paper. The thick grey line represents the outline of the Roer Valley Graben (after Kombrink et al., 2012).

to assess the spatial variation in lithologies and large-scale sedimentary structures.

2D palinspastic restoration

A 2D palinspastic restoration study was performed for six seismic transects in the Roer Valley Graben using the software MOVE (www.petex.com) in order to: i) investigate the deformation and burial history of the Main Buntsandstein and ii) reconstruct the basin geometry during the Early to Middle Triassic. Before restoring, each section was prepared by manually smoothing all the interpreted seismic horizons and removing faults without visible offset to avoid artifact occurrences during the restoration.

Additionally, a line-length balancing method was performed to validate the quality of the seismic interpretation. The approach assumes that horizon lengths do not change between deformed (present-day) and restored horizon lengths (Suppe, 1985; Lingrey and Vidal-Royo, 2016).

No effect of the Hardegsen unconformity on the lower Triassic sediments was observed in the seismic data. Therefore, seismic facies representing sediments of the Main Buntsandstein were grouped with seismic facies representing sediments of the Upper Germanic Trias Group (Solling, Röt, Muschelkalk and Keuper Formations). Furthermore, for simplicity, we assumed that the erosion related to the Mid- to Late Kimmerian tectonic phases occurred once the Schieland Group was deposited, as detailed
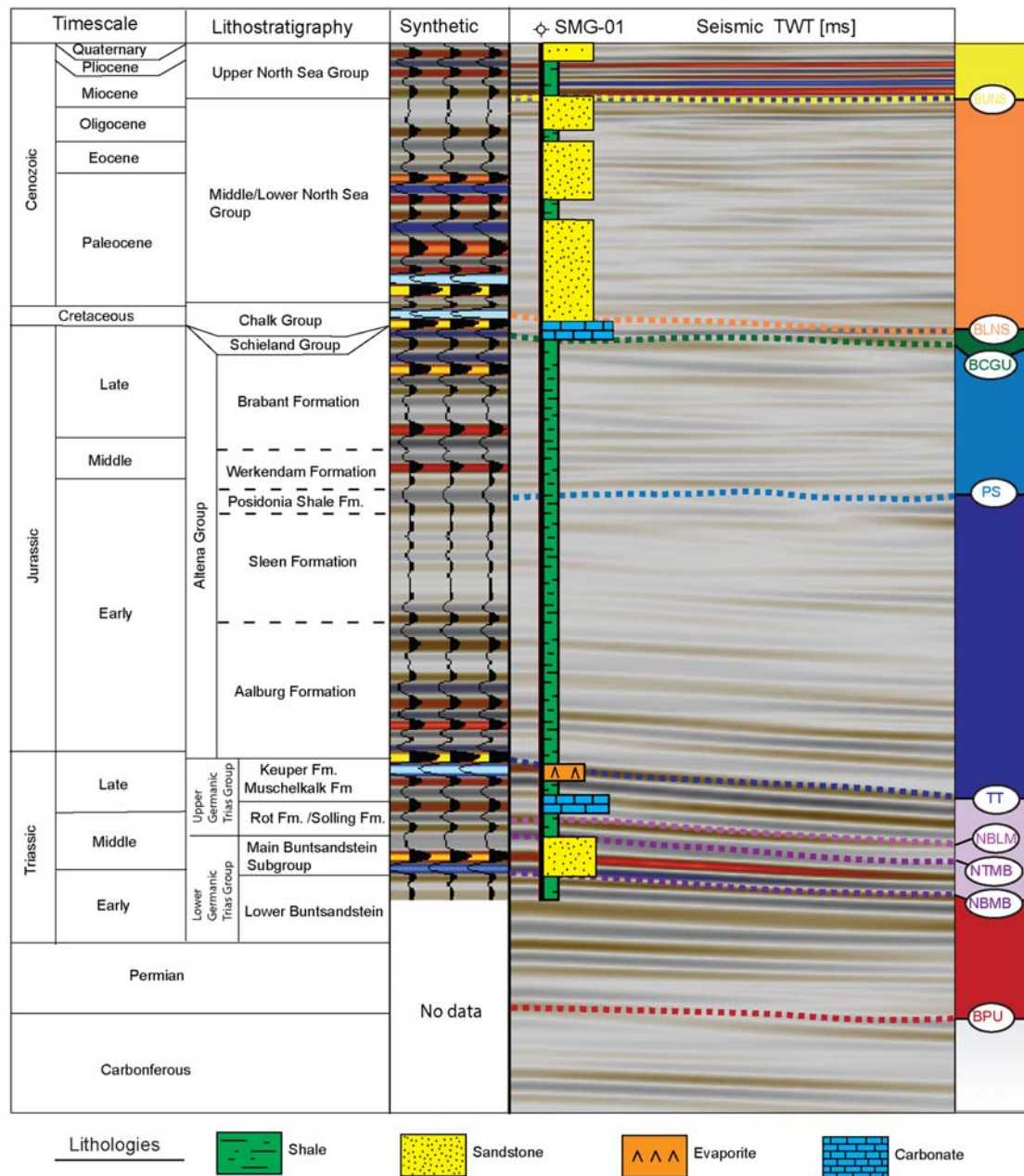
Figure 3. Seismic stratigraphy of the Roer Valley Graben. Lithological column after Van Adrichem Boogaert et al. (1993). The synthetic seismogram has been generated for well SMG-01 using a zero phase Ricker 25 Hz wavelet with length of 128 ms. The synthetic has been then tied to the reprocessed seismic line 81-08. See location of the well in Figure 6.

reconstructions of the tectonostratigraphic history of the Altena and Schieland Groups go beyond the scope of this paper.

During the restoration, horizon reconstructions were performed for the lithostratigraphic units eroded during Mesozoic tectonic events. The lithostratigraphic units that were reconstructed are Chalk Group, Schieland Group, Altena Group, Germanic Trias Group and the Permian units. The thickness of the individual lithostratigraphic units mapped in the area and available erosion maps (Nelskamp and Verweij, 2012) were used as a proxy for horizon reconstructions.

The first step of the restoration process consists in removing the youngest sedimentary layer and decompact the units underneath. Decompaction in MOVE accounts for isostatic changes and uses a compaction curve that assumes constant values of porosity and lithology assigned to each sedimentary layer. Lithologies for each lithostratigraphic unit were chosen following Van Adrichem Boogaert and Kouwe (1993). Average porosity values were taken from www.ThermoGIS.nl. Once the youngest layer was removed, the effect of faults was removed, and the top of the model was unfolded to a reference datum. The datum depends on the topography/bathymetry at the time of deposition of each sedimentary unit (Van Adrichem Boogaert and Kouwe, 1993; Nelskamp and Verweij, 2012). The restored horizons were finally used to create a map of the restored base of the Main Buntsandstein Subgroup, which helped assess the Early to Middle Triassic basin geometry.

Results

Interpreted horizons

In total, 10 horizons corresponding to stratigraphic group and formation boundaries were interpreted in seismic data across the Roer Valley Graben (Fig. 3). The horizons were named after the stratigraphic nomenclature used in the Netherlands (TNO-GDN, 2023). For the Triassic horizons, the adjective 'near' was added to the horizon names when their interpretation was uncertain. The uncertainties were caused by the low impedance contrast between reflectors and poor resolution of the seismic profiles at depths starting from below 2 km.

The shallowest interpreted horizons represent the bases of the Upper North Sea Group (BUNS) and Lower North Sea Group (BLNS). The boundary between the North Sea Supergroup and the underlying Chalk Group is generally sharp as a result of a change in lithology from the sandstones of the Lower North Sea Group to the carbonates of the Chalk Group. This produces a strong acoustic impedance contrast between the two units.

The carbonate rocks from the Chalk Group unconformably overly sediments ranging from Early Cretaceous (Berriasian) to carboniferous in age. This regional angular unconformity is referred to in this study as the base Chalk Group unconformity (BCGU). In the southeastern part of the Netherlands, the base Chalk Group corresponds to the base of the Oploo or younger formations as the Texel Formation is largely absent (TNO-GDN, 2023).

Below the base Chalk Group unconformity, a sequence of high-amplitude reflectors corresponds to the clastic deposits of the Schieland Group of which the base is separately mapped as the base Schieland Group (BS). The Schieland Group is only present in the northwest part of the Roer Valley Graben. The next high amplitude reflector is interpreted as the organic-rich Posidonia Shale showing a sharp density and velocity contrast with the overlying units. This horizon is present only in the central parts of the Roer Valley Graben, where it is used as reference to locate the underlying Triassic units.

The upper part of the Triassic units is characterised by a package of high-amplitude reflectors, reflecting acoustic imped-ance contrasts likely associated with anhydrite claystones of the Keuper Formation and argillaceous dolomites and limestones of the Muschelkalk Formation. The top of this package has been labelled as the top Triassic (TT), while the base has been interpreted as the near base Lower Muschelkalk. The near top and base of the Main Buntsandstein Subgroup (NTMB and NBMB, respectively) are usually characterised by weak reflections, reflecting the lack of a sharp density and velocity contrast with the overlying and underlying units. A detailed analysis of the Main Buntsandstein reflections is provided later in the text.

Below the Triassic horizons, a prominent angular uncon-formity is interpreted to represent the base Permian uncon-formity (BPU), separating Permian from carboniferous sediments. In the southeastern termination of the Roer Valley Graben (e.g. well RAA-01 in Fig. 2), Permian deposits are absent, and consequently, the Triassic succession directly overlies carboniferous deposits.

Seismic mapping

Two transects are shown to illustrate the architecture of the Roer Valley Graben and the Main Buntsandstein Subgroup distribution across the area. The first is oriented WSW-ENE (Fig. 4) and

roughly perpendicular to the main trend of faults in the Roer Valley Graben; the second one is oriented SE-NW (Fig. 5) and semi-parallel to the Roer Valley Graben axis. Both transects will be described in more detail below.

Semi-perpendicular to the Graben axis section

The preservation of the Main Buntsandstein sediments in the Roer Valley Graben is limited by a series of normal faults separating the Roer Valley Graben from the adjacent highs, the Zeeland High and the Peel-Maasbommel Complex (e.g. F14 and F2 in Fig. 4). Beyond these faults, the Main Buntsandstein sediments are truncated at the base Chalk Group unconformity (Fig 4b). The Main Buntsandstein reflector package displays a sheet-like external shape, with reflector configuration changing from parallel/sub-parallel to chaotic from WSW to ENE (Fig. 4c).

The Main Buntsandstein is encountered at its greatest depths in the central part of the Roer Valley Graben. Here, depths of 4 km are locally exceeded and reflectors appear semi-horizontal (Fig. 4b and c). Towards the flanks, the Main Buntsandstein sediments are shallowing up to just below 1 km (Fig. 4a) and dip basinwards as a result of faulting and tilting (Fig. 4c). Along both flanks of the Roer Valley Graben, two sub-basin structures are present (Fig. 4c). These two structures are bounded by normal faults labelled F2 and F6 for sub-basin 1 and F12 and F13 for sub-basin 2. These sub-basins define areas where the Main Buntsandstein Subgroup is present around 100–500 m deeper than in the adjacent blocks (Fig. 4c).

Several faults are recognised along the WSW-ENE seismic section, mostly with a normal slip character. The faults bounding the Roer Valley Graben yield the largest vertical offset, displacing the Main Buntsandstein sediments by ~700–800 m (e.g. F2 and F13 in Fig. 4) and laterally juxtapose Triassic to Jurassic and carboniferous units. These faults affect the lateral continuity of the Triassic units, reducing the lateral extent of the Main Buntsandstein sediments locally to less than 2 km in certain areas along the section strike (Fig. 4c). These large boundary faults separate the Roer Valley Graben from the adjacent platform areas, where the Main Buntsandstein sediments are found at depths of 1000–1500 m and are locally truncated at the base Chalk Group unconformity (Fig. 4c).

Overall, the Main Buntsandstein Subgroup thickens southwest-wards, where the wells BKZ-01 and HVB-01 record thicknesses of 250 m. This thickening is enhanced by the presence of syn-sedimentary fault activity (e.g. F7 in Fig. 4b). In the central part of the Roer Valley Graben, four more syn-sedimentary faults have been interpreted where the Buntsandstein sediments display a change in thickness in the order of tens of meters across the fault plane (Fig. 4c).

Small reverse faults occur within the two sub-basin structures displacing the overlying Jurassic horizons of ~30–40 m (e.g. F5, F7 and F9 in Fig. 4b). Further to the north, reverse faults are instead cross-cutting the Triassic units and reducing their lateral extent (Fig. 11). No faults have been mapped below the Base Permian unconformity due to the low seismic resolution of these deeper strata. As a consequence, the continuation of faults at depths greater than 2 to 3 km is uncertain and marked with a dashed line in the figures.

Semi-parallel to the Graben axis section

In the southeastern part of the Roer Valley Graben, the Main Buntsandstein reflectors are mostly continuous at km-scale, with a dominant parallel/sub-parallel configuration. Nevertheless, reflec-tors lose continuity in an area where the configuration changes
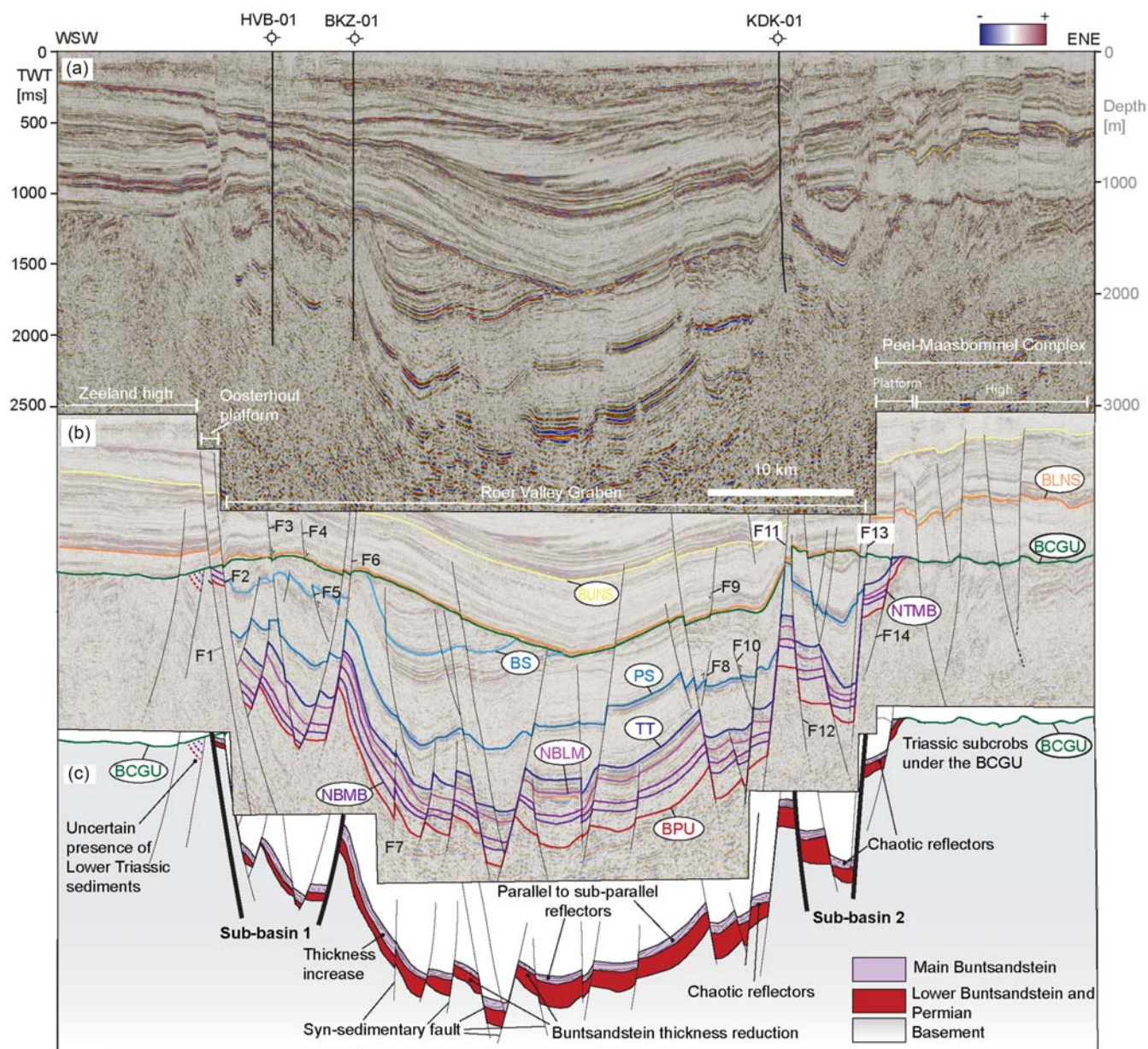
Figure 4. Un-interpreted (a) and interpreted (b–c) seismic section EBN017-EBN018. The horizon colours refer to specific stratigraphic units (see Fig. 3). Only the main faults are interpreted in the section. Some of these faults have been numbered to refer to in the text. See Fig. 2 to see location of the seismic section.

from parallel/sub-parallel to chaotic and Mesozoic deposits could not be mapped (Fig. 5c). An absence of wells in that area prevent to discern whether that is a structural high, where Mesozoic sediments have not been deposited or preserved, or it is a large fault shadow that creates these seemingly chaotic reflections (Fig. 5c).

To the northwest, detailed mapping of the Main Buntsandstein was not possible due to a low resolution of the seismic data below 1500 m and a larger number of faults compared to the southern part of the seismic section (Fig. 5c). Nonetheless, the configuration of reflectors below the top Triassic in the northwestern area appears to be more chaotic and their overall continuity being reduced by faulting with respect to the southeastern part of the Roer Valley Graben.

Overall, the Main Buntsandstein Subgroup sediments are present at depths below 2 km in the southeastern part of the Roer

Valley Graben, while they deepen reaching 3.5–4 km near the Graben axis (Fig. 5c). In the southeastern part of the Roer Valley Graben, a 50–100 m succession of Jurassic units separates the Triassic sediments from the overlying base Chalk Group unconformity (Fig. 5b and c). Locally, normal faulting juxtaposes the Main Buntsandstein to the upper Triassic, Jurassic and Carboniferous units, as exemplified by F4, F5 and F7 in Fig. 5c. To the southeast, a series of normal faults display sediments up to Cenozoic in age (e.g. F4 and F8 in Fig. 5b). These faults represent the furthest southeastern margin of the Roer Valley Graben and yield normal displacements of up to ~200–300 m.

Main Buntsandstein depth and gross thickness maps

The depth map of the near base Main Buntsandstein is calculated by integrating data from all wells and interpreted seismic profiles.
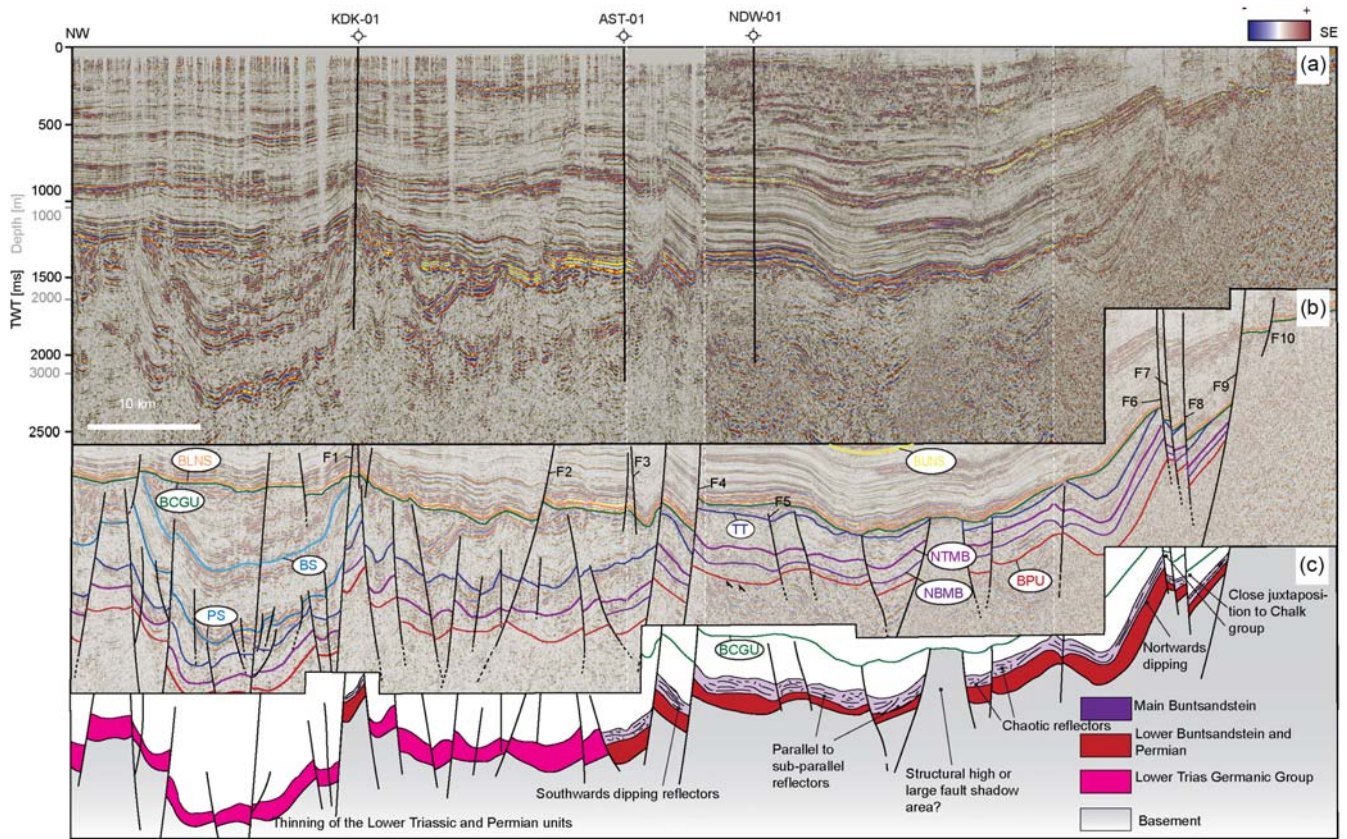
Figure 5. Un-interpreted (a) and interpreted (b–c) composite line partially along the basin axis realized merging together the following transects: EBN031, EBN030, 80-3 and 81-17. Colours refer to specific stratigraphic units (see Fig. 3). The seismic imaging in the left part of the transect is of poor quality, thus the interpretation of the Main Buntsandstein was not always possible. For the location of the composite line see Fig. 2.

The map shows that the base of the Main Buntsandstein deepens from the flanks to the centre of the Roer Valley Graben (Fig. 6a). To the northeast of Tilburg, the base of the Buntsandstein locally reaches depths of ~4 km (Fig. 6a). In the southeastern part of Roer Valley Graben, the base of the Main Buntsandstein shallows up to 2–3 km. In the platform areas that separate the Roer Valley Graben from the adjacent highs where the Buntsandstein is absent, the depth of the Main Buntsandstein is largely found between 1 and 2 km (Fig. 6a). These areas have a width from ~1 to 15 km (Fig. 6a). To the southeast, the Roer Valley Graben is narrower (~27 km) compared to the northern part (~45 km), which reflects a reduction of the area where the Main Buntsandstein sediments are preserved (Fig 6b; see also Appendix Fig. S2).

The thickest preserved Main Buntsandstein succession, called Main Buntsandstein gross thickness in Fig 6b, is located between the cities of Tilburg and Eindhoven, where the thickness locally reaches values up to 300 m (Fig. 6b). In this area, the presence of thickness variations across fault planes indicates syn-sedimentary fault activity (e.g. F7 in Fig. 4c). The thickness decreases to the northwest, where well STH-01 records a thickness of ~125 m for the whole Main Buntsandstein. This well is located in the Oosterhout Platform, where the Main Buntsandstein occurs shallower at depths of ~1000–1500 m (Fig. 6a). The Main Buntsandstein overall thins towards the northern flank of the Roer Valley Graben where thicknesses of 100–150 m are recorded. In the southeastern part of the Roer Valley Graben, the Main Buntsandstein Subgroup thickness reaches values over 200 m. However, the presence of only two wells penetrating the Main

Buntsandstein in this part of the study area makes the thickness quantification more uncertain.

Main Buntsandstein reflector characterisation

From south to north, the Main Buntsandstein Subgroup reflectors show variations in amplitude, frequency and wavelet geometries. The change in reflector character is illustrated through six seismic profiles, three located south of the city of Eindhoven (Figs. 7, 8 and 9) and three located in the area north of Eindhoven (Figs. 10, 11, and 12).

Southern area

In the southeastern part of the study area, the top and base of the Main Buntsandstein are laterally continuous, marked by low amplitude reflectors that can be correlated for over 5 km (Fig. 7a). Such continuity results in a sheet-like external shape without major lateral variation in thickness. Around NDW-01, top and base Main Buntsandstein continuity is interrupted by faults (e.g. F5 in Fig. 5). Internally, reflectors display a parallel to subparallel configuration with overall low amplitudes and minor frequency variation (Fig. 7b and c). Reflectors are mostly vertically aggrading; nonetheless, downlap terminations have been mapped (Fig. 7b). Local increases in reflector amplitudes at the top of the Main Buntsandstein units seem to represent velocity contrasts as a result of changes in lithology and bed thickness from the lower to the upper part of the Main Buntsandstein, as exemplified by the lithological log in NDW-01 (Fig. 7a and b).
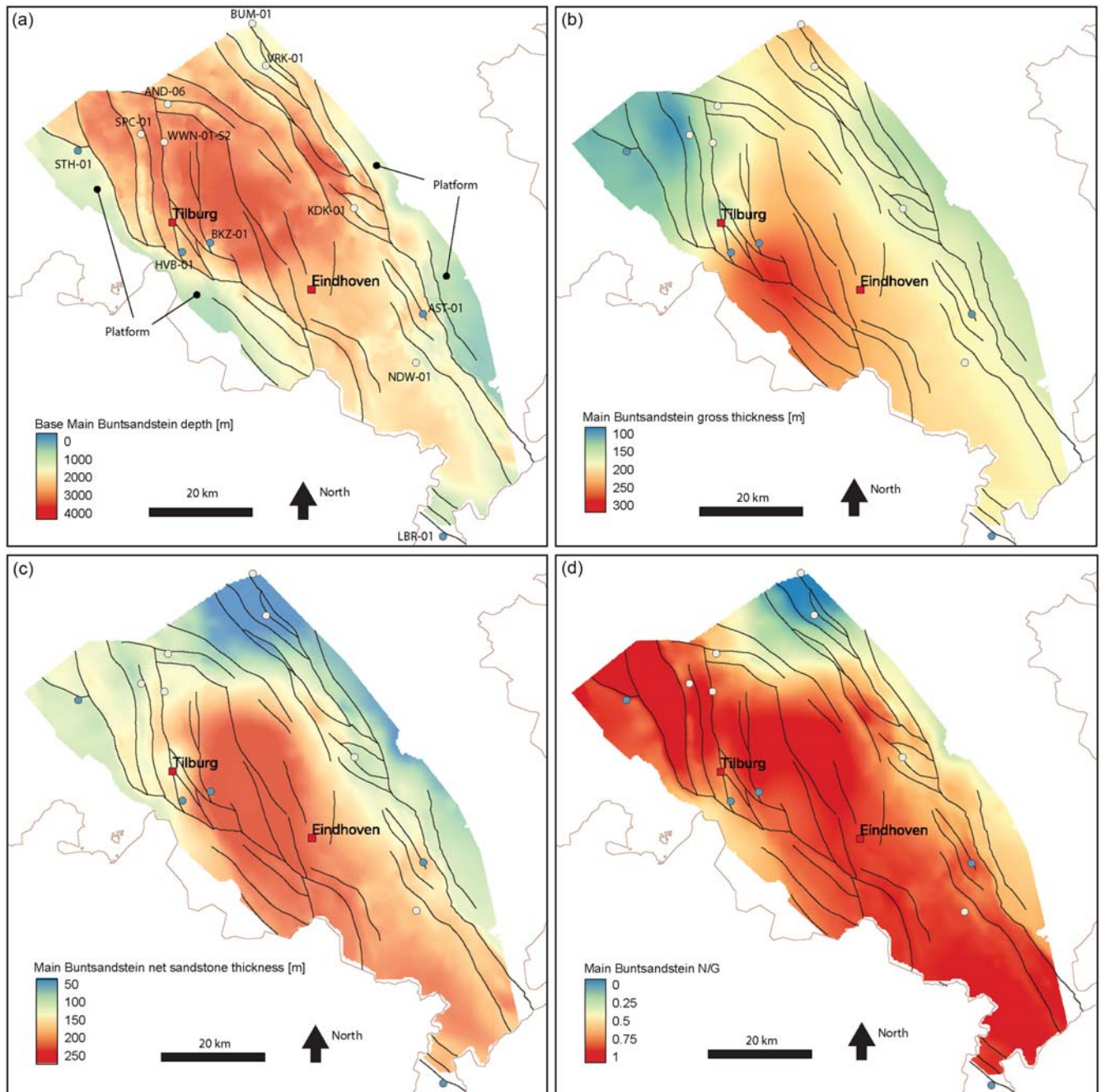
Figure 6. a) Structural depth in meters of the near base Main Buntsandstein. b) Gross thickness in meters of the Main Buntsandstein. c) Net sandstone thickness in meters for the Main Buntsandstein. d) Net to gross ratio. Black continuous lines represent faults mapped after TNO Digital Geological Model (https://www.dinoloket.nl/en/the-digital-geological-model-dgm).

Moving towards the northern flank of the Roer Valley Graben, the geometry of the reflectors becomes more heterogeneous, with configurations alternating between parallel to sub-parallel and chaotic, toplap terminations and variable amplitudes (Figs. 8c and 5). The reflector at the base of the Main Buntsandstein reflector sequence remains continuous over 5–6 km, while the reflector at the top becomes more discontinuous with higher amplitudes and frequencies.

Along the southwestern flank of the Roer Valley Graben, the top of the Main Buntsandstein is marked by a high amplitude reflector that is continuous at km scale and locally disrupted by

the presence of small normal faults (Fig. 9a and b). The base of the Main Buntsandstein has lower amplitude reflectors that are continuous at km scale. Internally, the Main Buntsandstein reflector geometry changes from prograding downlapping reflections to chaotic and parallel/sub-parallel (Fig. 9c). The prograding reflectors form a package approximately 100 m thick and about 1 km wide before pinching out to the northwest (Fig. 9c). To the southeast, chaotic reflectors are observed as infilling on a slope-like geometry. Internal, parallel to sub-parallel reflectors are aggrading, losing continuity over 1–2 km.
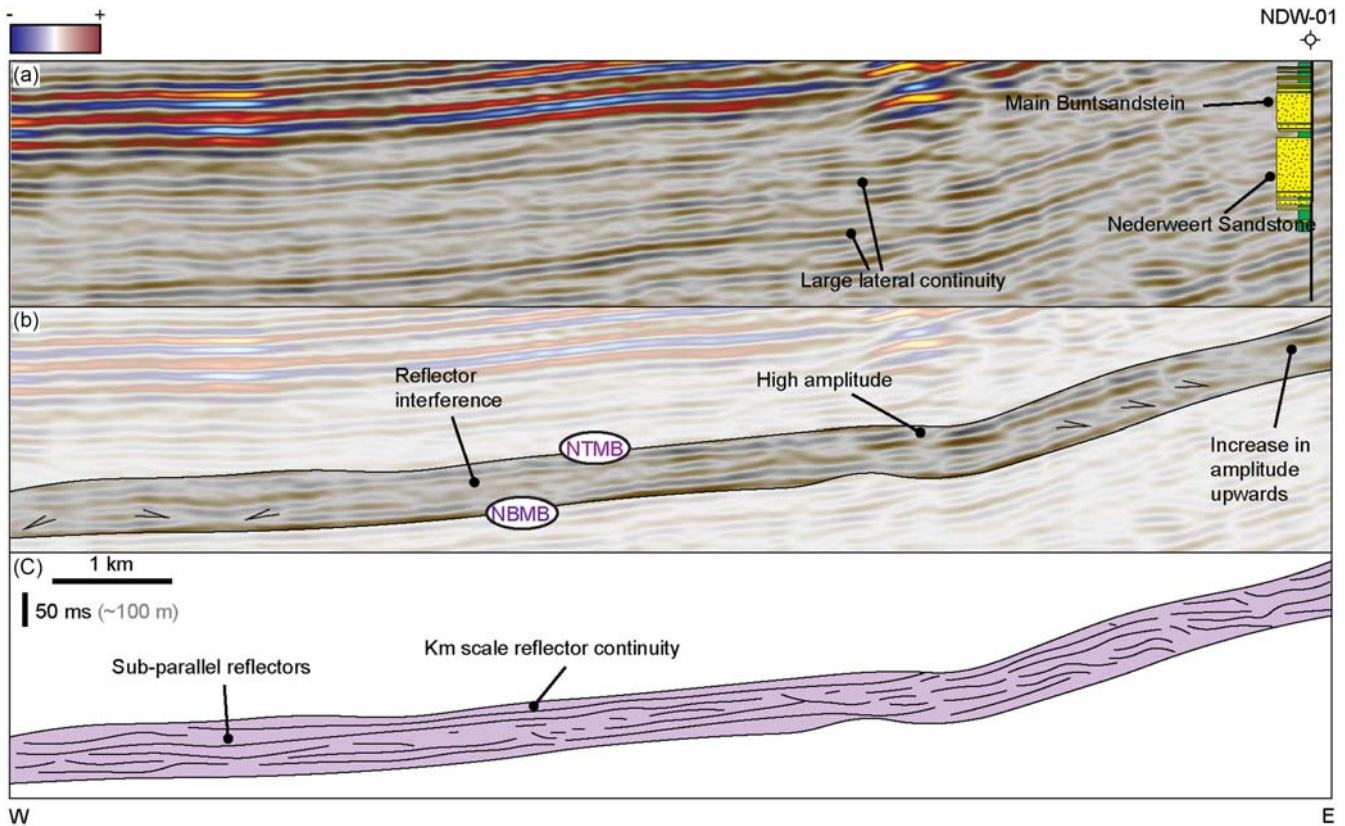
Figure 7. Uninterpreted (a) and interpreted (b–c) 2D seismic profile 82-11 (see location on Fig. 2) showing the main geometries in the Main Buntsandstein observed around NDW-01. A schematic lithological log is displayed along the well track of NDW-01, where sandstone intervals are coloured in yellow and claystone intervals in green. The sandstone units below the Main Buntsandstein are classified as the Nederweert Sandstone.
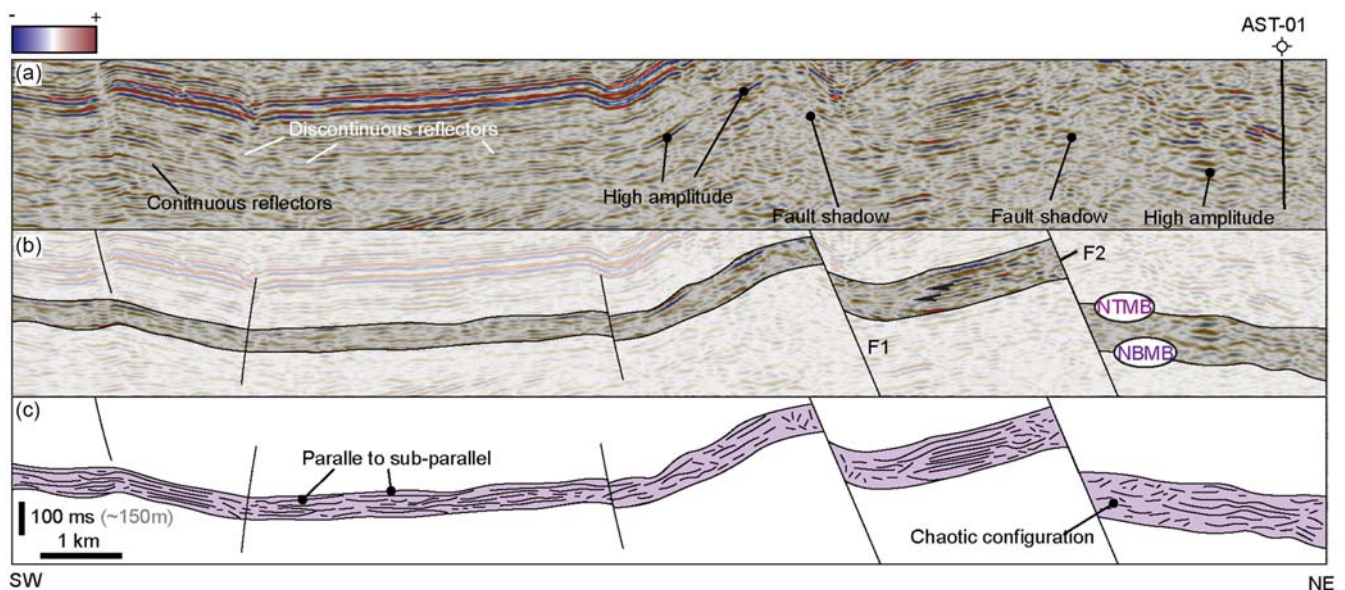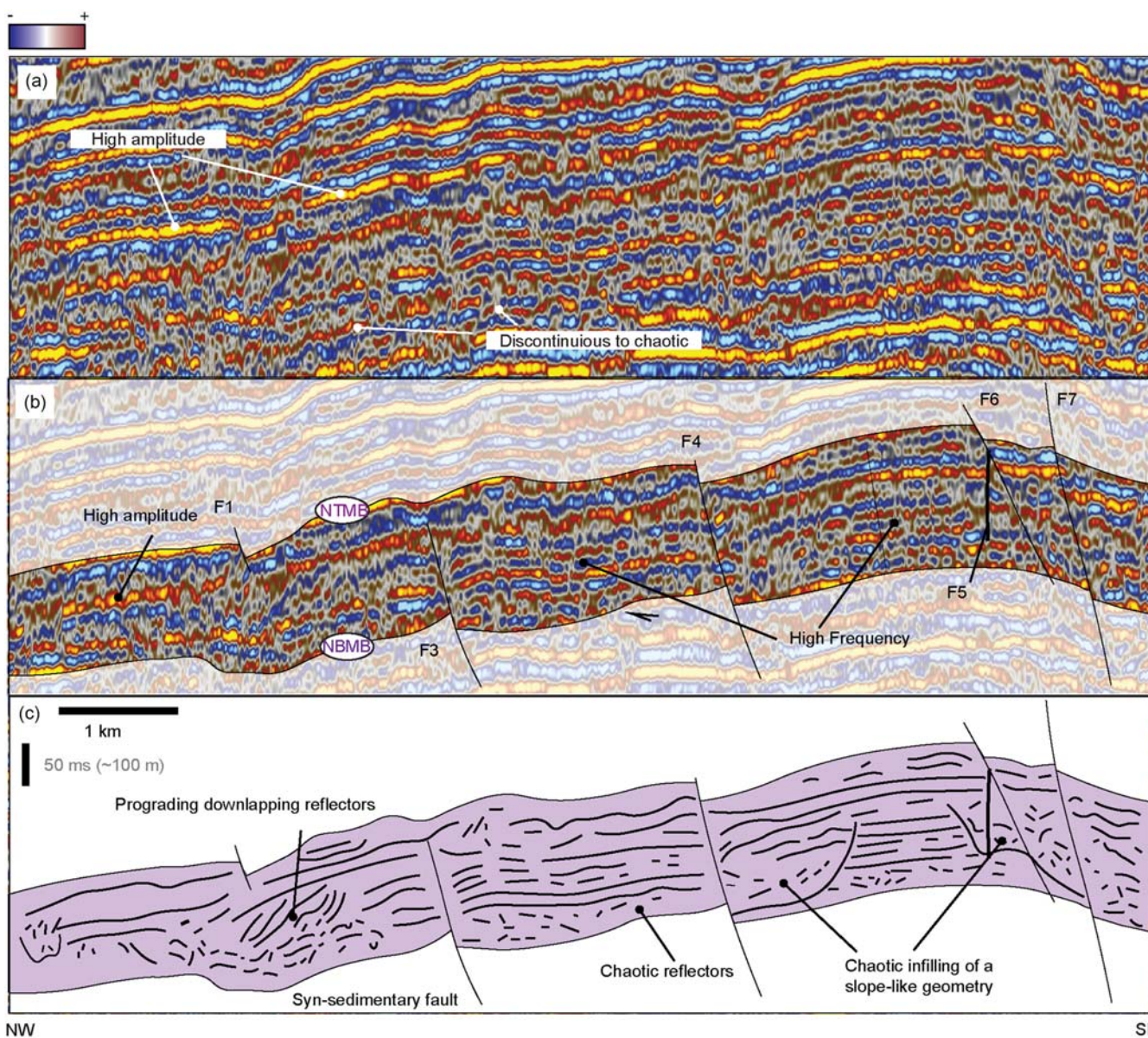

Figure 8. Un-interpreted (a) and interpreted (b–c) 2D seismic profile 80-03 (see location on Fig. 2) showing the main geometries in the Main Buntsandstein observed around AST-01. See text for detail description of the seismic profile.

Northern area

In the northwestern part of the Roer Valley Graben, the top and base of the Main Buntsandstein are marked by discontinuous low-amplitude reflectors (Fig. 10a). In the Oosterhout Platform, high-amplitude reflectors at the base and the top of the Main

Buntsandstein seem to reflect a decrease in N/G, as exemplified by the lithological log of well STH-01. Overall, the lateral continuity of the Main Buntsandstein reflectors is reduced to less than 1 km. These reflectors display parallel to sub-parallel configurations and less frequently more chaotic configurations (Fig. 10c). To the

Figure 9. Un-interpreted (a) and interpreted (b–c) 2D seismic profile 81-12 (see location on Fig. 2) showing the main geometries in the Main Buntsandstein along the southwestern margin of the study area. See text for detail description of the seismic profile.

northwest, the Main Buntsandstein reflectors subcrop beneath the base Chalk unconformity, where upper Triassic and Jurassic sediments are not preserved.

Towards the north, the area around well VRK-01 is dominated by chaotic reflections with low to medium amplitudes (Fig. 11c). Combining the lithological information from VRK-01 with the geometry of the observed reflectors, chaotic reflections are likely to be the product of fine-grained clastic sediments with occasional conglomeratic deposits as observed in the core pictures of VRK-01 (www.nlog.nl).

Further to the north, reflections near well BUM-01 are characterised by overall high frequencies and amplitudes, likely reflecting the alteration of sandstones and claystones in the lithological log (Fig. 12a). Unfortunately, the presence of a fault shadow zone in the footwall of F2 does not allow a direct tie between the seismic reflectors and the well (Fig. 12a and b). In the hanging wall, the top of the Main Buntsandstein is marked by a high-amplitude reflector of which the continuity is laterally interrupted by the presence of faulting (F1 and F2 in Fig. 12b). Conversely, the base is marked by a chaotic reflection configuration.

Net sandstone thickness and N/G maps

Net sandstone thickness and net-to-gross (N/G) maps display the distribution of the Main Buntsandstein across the Roer Valley Graben and its immediate surroundings. The thickest sandstone sequences have been deposited in the central and southeastern part of the study area, with local maxima up to 250 m in between the cities of Tilburg and Eindhoven (Fig. 6c). In this area, reflectors are mostly continuous at km-scale, with an overall low amplitude indicating rather homogeneous lithologies. The northern part of the study area is dominated instead by the deposition of fine-grained sediments and displays a net sandstone thickness of locally
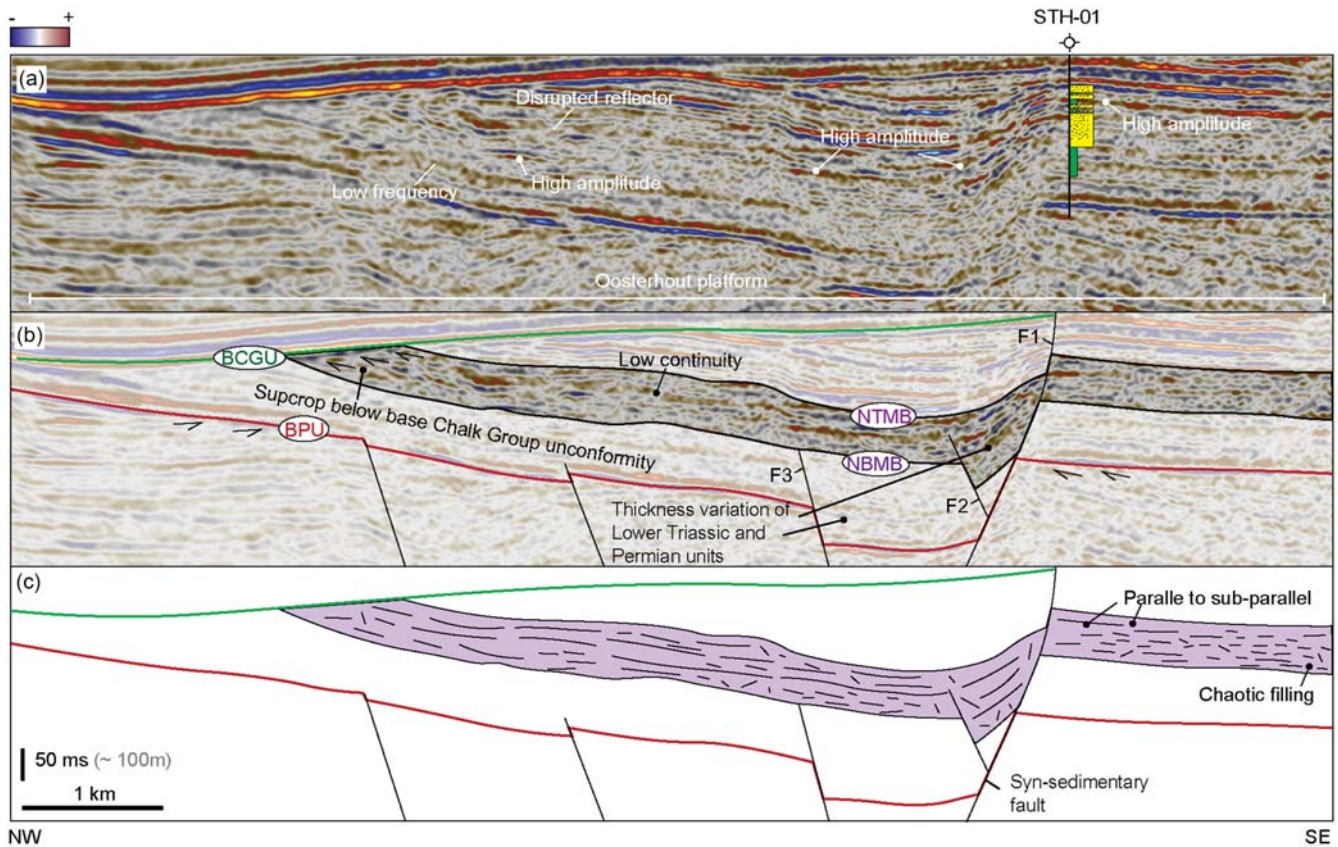
Figure 10. Un-interpreted (a) and interpreted (b–c) 2D seismic profile EBN033 (see location on Fig. 2) showing the main geometries in the Main Buntsandstein around STH-01. A schematic lithological log is displayed along the well track of STH-01, where sandstone intervals are coloured in yellow and claystone intervals in green.

less than 50 m. This trend is best displayed by a decrease in N/G from south to north, where the area around wells BUM-01 and VRK-01 show the highest percentages of fine materials (Fig. 6d). Along with this fining trend, the seismic reflection character shows a decrease in reflector continuity and increase in amplitudes northwards while also chaotic configurations become more dominant compared to parallel or subparallel configurations. To the northwest, the net sandstone thickness decreases to 100 m around well STH-01, while the N/G is still above 0.75.

Sequential restoration

The deformation and burial history of the Main Buntsandstein Subgroup in the Roer Valley Graben and adjacent areas can be split into four main stages: i) Main Buntsandstein deposition and initial burial during an extensional regime characterised by the normal faulting throughout the Triassic and the Middle Jurassic (Fig. 13 g and f); ii) a Late Jurassic to Early Cretaceous local uplift, truncation and erosion responsible for the absence of the Main Buntsandstein on the Roer Valley Graben flanks (Fig. 13 e); iii) uplift of the central parts of the Roer Valley Graben and subsidence of its flanks during the Late Cretaceous basin inversion (Fig. 13d and e); iv) a second phase of extension and sedimentation of Cenozoic sediments in the Roer Valley Graben and to limited extent on its flanks (Fig. 13a, b and c).

The restored section indicates that there is a thickening of the middle to upper Triassic units to the southwest (Fig. 13g). This is caused by syn-sedimentary faulting in this part of the Roer Valley

Graben (Fig. 4c). After deposition, the Main Buntsandstein sediments were continuously buried until Jurassic times. Once the marine Altena and terrestrial Schieland Groups were deposited, the base of the Main Buntsandstein Subgroup was buried down to ~3–3.5 km in the central parts of the Roer Valley Graben (Fig. 13g). This burial depth decreased down to ~2.5 km towards the southern flank of the Roer Valley Graben (Fig. 13g), where a thinner Jurassic sequence with a thickness of ~2 km was likely being deposited.

During Late Jurassic to Early Cretaceous times, the Roer Valley Graben flanks were affected by widespread uplift and erosion, which largely removed the Jurassic, Triassic and Permian units, especially in the Peel Complex, Zeeland High and Oosterhout Platform (Fig. 13f). The uplift and erosion were likely driven by the activity of the large faults that bound the Roer Valley Graben (e.g. F2 and F13 in Fig. 4b). In parallel, fault movements within the Roer Valley Graben produced a horst and Graben geometry, with the development of sub-basin structures (e.g. sub-basins 1 and 2 in Fig. 4). At this stage, the Main Buntsandstein sediments were buried at depths ranging between ~2 and 3.5 km in the central part of the Roer Valley Graben (Fig. 13e). The burial depths gently decreased across the areas adjacent to the Roer Valley Graben, where the Main Buntsandstein sediments were encountered closer to the surface as result of the erosion of the overlying Jurassic and Cretaceous units (Fig. 13e and Fig. S4d in the Appendix).

Subsequently, a sequence of Chalk was deposited across the Roer Valley Graben area on top of Early Cretaceous or older sediments, developing an angular unconformity that is referred to in this work as the base Chalk Group unconformity (Fig. 3).
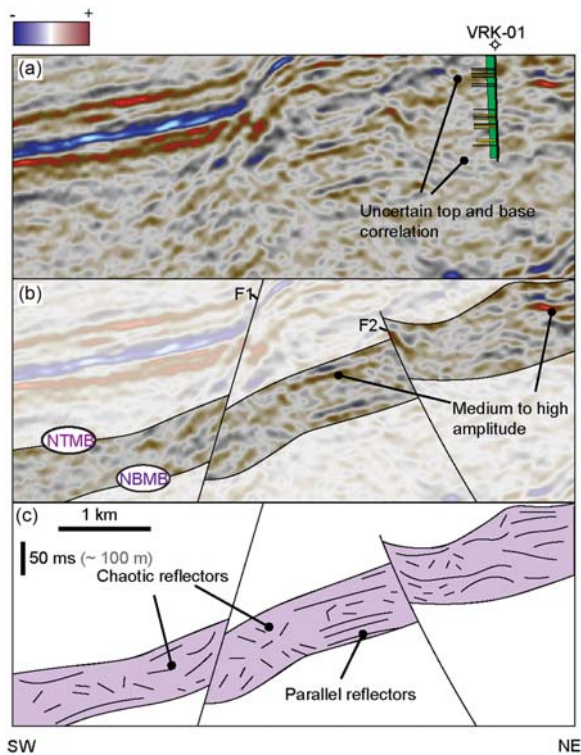
Figure 11. Un-interpreted (a) and interpreted (b–c) 2D seismic profile 872104 (see location on Fig. 2) showing the main geometries in the Main Buntsandstein around VRK-01. A schematic lithological log is displayed along the well track of VRK-01, where sandstone intervals are coloured in yellow and claystone intervals in green.

Sediments from the Chalk Group are thinner in the Roer Valley Graben compared to the adjacent platforms and highs. This is caused by the inversion of some of the faults along the flanks of the Roer Valley Graben after the deposition of the Chalk Group. The inversion of these faults resulted in the uplift and the widespread erosion of Chalk sediments in the Graben area. In contrast, the Chalk sediments were preserved along the flanks, which continued to subside at this time.

The inverted faults display normal offset in the lowermost tracts, while they show reverse displacement in the upper portion of the fault, a diagnostic feature of fault inversion (Williams et al., 1989). The inversion seems also to propagate across the Lower North Sea Group (Fig. 13c).

The last burial phase lasts until present-day, and the sediment infill causes the base of the Main Buntsandstein to be buried locally below 4 km (Fig. 13a and b). During this phase, the Roer Valley Graben represents the main subsiding area where ~1500 m of North Sea Supergroup sediments have been deposited, while a thinner sequence (500-1000 m) of North Sea Supergroup sediments is present in the blocks adjacent to the Roer Valley Graben.

Discussion

Structural evolution of the Roer Valley Graben

The presence of syn-sedimentary faults producing thickness variation in the Main Buntsandstein sediments (e.g. F1 and F2 Fig. 10b) indicates that the Roer Valley Graben was tectonically active during Early to Middle Triassic times. These faults are

normal and oriented ~NW–SE, producing depocenters for sedimentation on their hanging walls. The Main Buntsandstein Subgroup is thus interpreted to represent a syn-rift sequence, where the thickness of the syn-rift infill increases in the area around Eindhoven and southeast of Tilburg. The syn-sedimentary faults observed in the Roer Valley Graben could be related to larger NW-SE fault complexes along the northern margin of the London-Brabant Massif that were active during Early to Middle Triassic times (Geluk, 2005). This rift developed contemporaneous with the Permo-Triassic rifting stage affecting the North Sea area (Fossen et al., 2021). The lack of internal unconformities within the Triassic sediments in the seismic interpretations supports the absence of the Hardegsen unconformity in Graben systems such as the Roer Valley Graben (Mckie, 2011).

During Jurassic to Early Cretaceous times, our palinspastic restoration shows that the Main Buntsandstein sediments have been buried up to 3.5 km depth in the central part of the Roer Valley Graben in response to regional extensional tectonics (Ziegler, 1992; Geluk, 2007). The present-day occurrence of the Altena and Schieland Group sediments in the central part of the basin and their partial absence in the adjacent platforms and highs indicate that these blocks were subjected to different degrees of subsidence. During Jurassic times, the Main Buntsandstein experienced a shallower burial depth (~2–2.5 km) in the southern platform areas compared to the deeper burial depths experienced by the Main Buntsandstein sediments in the blocks located in the central Graben areas (e.g. Fig. 13f; see also Appendix Fig. S4e).

Carter et al. (1990) indicate the Main Buntsandstein reached maximum burial depths of ~2.5 km during the Jurassic, in the wells located in the northern part of the Roer Valley Graben. In this work, we assume that the Altena and Schieland Groups were largely deposited across the Roer Valley Graben and on the adjacent platforms and highs. However, our horizon reconstruction was performed based on the thicknesses observed in the central parts of Roer Valley Graben, where Jurassic sediments are preserved and thickest. This assumption may have resulted in an overestimation of the burial depths in areas where, instead, a thinner Jurassic sedimentary sequence was deposited (Fig. 13f).

The sediments in the Roer Valley Graben were subsequently eroded during the Middle to Late Jurassic in response to the Mid-to Late-Kimmerian tectonic phases that caused the formation of a series of faults responsible for the creation of sub-Graben systems within the Roer Valley Graben (e.g. sub basins 1 and 2 in Fig. 4) and the uplift of the adjacent block terrains (Vercouter and Van de Haute, 1993; NITG, 2004; Deckers et al., 2023). This uplift resulted in the deep truncation and erosion of Mesozoic sediments across the Roer Valley Graben flanks and the development of areas where Triassic sediments are now truncated at the base Chalk Group unconformity (Figs. 4 and 5).

The platforms are the areas along the Roer Valley Graben flanks where the Main Buntsandstein sediments are usually present at depths shallower than 1500–2000 m and locally subcrop at the base Chalk Group unconformity and (e.g. Fig. 4). These platforms are narrowest on the southeast termination of the Roer Valley Graben, where the Main Buntsandstein is mostly absent on the blocks adjacent to the Roer Valley Graben (Fig. S2c Appendix). The base Chalk Group unconformity represents an angular unconformity that developed as the result of fault inversion along the flanks of the Roer Valley Graben. Palinspastic restoration analysis displayed how the thicker deposition of the Chalk Group on the platforms
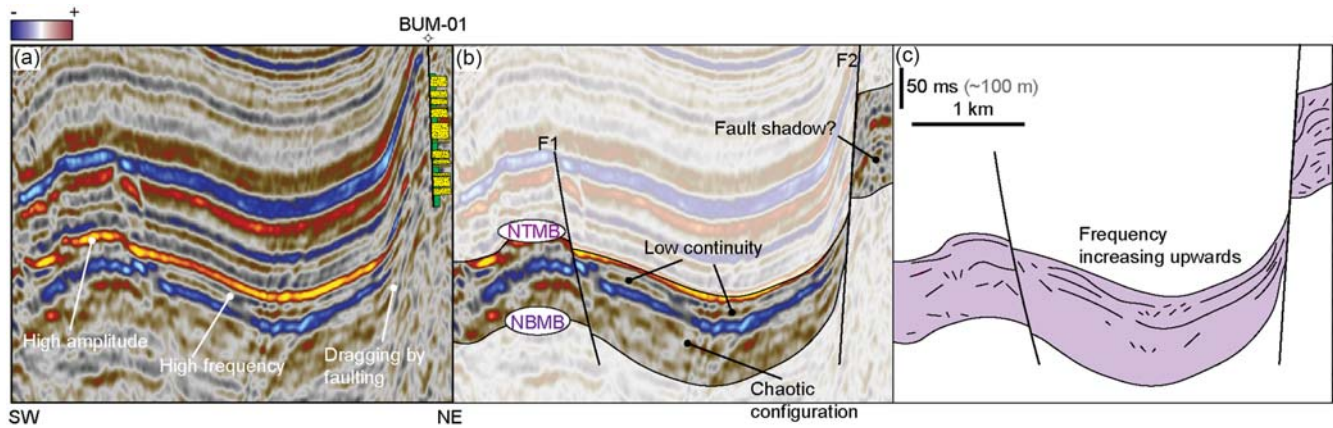
Figure 12. Un-interpreted (a) and interpreted (b–c) 2D seismic profile EBN003 (see location on Fig. 2) showing the main geometries in the Main Buntsandstein around BUM-01. A schematic lithological log is displayed along the well track of BUM-01, where sandstone intervals are coloured in yellow and claystone intervals in green.

and highs is associated with fault inversion, reflected by faults displaying normal offset in their lower tracts and reverse displacement in their upper portion. In this context, sediments were mostly deposited on the fault footwalls, while the hanging walls were mostly affected by erosion. This is aligned with previous studies on the tectonic history of the Roer Valley Graben area (Geluk et al., 1994; Deckers et al., 2023). The reactivation of normal faults as reverse faults indicates the control exerted by pre-existing faults on the Roer Valley Graben deformation history (Deckers et al., 2021). This event is mostly evident in the northern part of the Roer Valley Graben as exemplified by the decrease in reverse fault occurrences further to the south (Fig. S3 in the Appendix).

After the Late Cretaceous inversion, the Roer Valley Graben was affected by an extensional regime that continues today (Geluk et al., 1994; Deckers et al., 2023). This is indicated by the presence of border faults that cut through the North Sea Supergroup sediments. These faults are well developed across the central and southern parts of the Roer Valley Graben, creating accommodation space filled with a thick coverage of Cenozoic sediments. This event buried the Main Buntsandstein sediments down to 4–4.5 km in the central part of the Roer Valley Graben, where they reach maximum burial depths confirming the results of previous burial history studies (Zijerveld et al., 1992; Nelskamp and Verweij, 2012).

Controls on the Early to Middle Triassic depocenter activity

The restored 2D transects allow to reconstruct the basin geometry and to evaluate the presence of depocenters at the time of deposition of the Main Buntsandstein (Fig. 14). By integrating these data with the reflector characteristics, sandstone thickness and N/G maps, the Main Buntsandstein fluvial sedimentary system in the Roer Valley Graben can be discussed.

During the Early to Middle Triassic, the central and southern parts of the Roer Valley Graben that extends from wells BKZ-01 to and beyond NDW-01 appeared to be a preferred sandstone depocenter considering the sandstone thicknesses recorded (Fig. 6c). These depocenters were likely produced by faults that were interpreted as active during the Early to Middle Triassic times (e.g. F7 in Fig. 4b). This is aligned with sediment dispersal patterns in a half-graben system associated with fluvial sedimentation, where the coarse-grained facies are likely to be located close to active faults or along the basin axis (Gawthorpe and Leeder, 2000). In the central and southeastern parts of the Roer Valley Graben, the

Main Buntsandstein reflectors show high continuity, locally over 5–7 km, and low amplitudes (e.g. Figs. 7, 8, and 10). The average high continuity and low amplitude suggest a great lateral extent of the same sedimentation conditions and rather homogeneous lithologies (Veeken and Van Moerkerken, 2013; Zeng, 2018). This is further supported by the average high N/G values in these parts of the Roer Valley Graben.

To the northwest, the overall decrease in the Main Buntsandstein gross and net sandstone thickness (Fig. 6b and c) and the presence of syn-sedimentary faults (Fig. 10) suggest the presence of an area where a lower subsidence rate in the footwall of active faults may have resulted in the deposition of a thinner Main Buntsandstein sequence (~125 m) as recorded in well STH-01. On the other hand, southeast of STH-01, a depocenter is displayed in the reconstructed basin geometry and confirmed by a Main Buntsandstein thickness of 250 m in well BKZ-01, where a higher subsidence rate may have enhanced the deposition of a thicker Main Buntsandstein sequence (Fig. 14).

To the northern edge of the study area, an increase in reflector amplitudes exemplifies the frequent lithological contrasts between sandstones and claystones observed in the available wells (e.g. Fig. 13a). In the Roer Valley Graben, fluvial sandstones pinch out northwards into playa-lake claystones (Geluk, 2005). The change in reflector characteristics in the northern part of the Roer Valley Graben and the lower N/G values in BUM-01 and VRK-01 suggest that these wells are in a more marginal area close to the southern edge of the Central Netherlands swell where mostly fine particles were delivered (Geluk and Röhling, 1997).

At the time of the deposition of the Main Buntsandstein, the London Brabant Massif was cropping out with an elevation of 2–3 km feeding sediments to the Roer Valley Graben (Carter et al., 1990; Köppen and Carter, 2000; Olivarius et al., 2017). Unfortunately, the widespread erosion of the Triassic layers on the Zeeland High does not allow to define the southern limit of the Main Buntsandstein deposition. However, the presence of a depocenter along the southern margin of the area may reflect the presence of fault activity along the northern margin of the London-Brabant Massif during the Early to Middle Triassic, where the Main Buntsandstein sediments from the London-Brabant Massif may have been deposited before being eroded during later tectonic events (Geluk et al., 1994; NITG, 2004; Kombrink et al., 2012).

The Roer Valley Graben represents the fareway for sediments from the Armorican Massif to enter the Germanic Basin (Geluk,
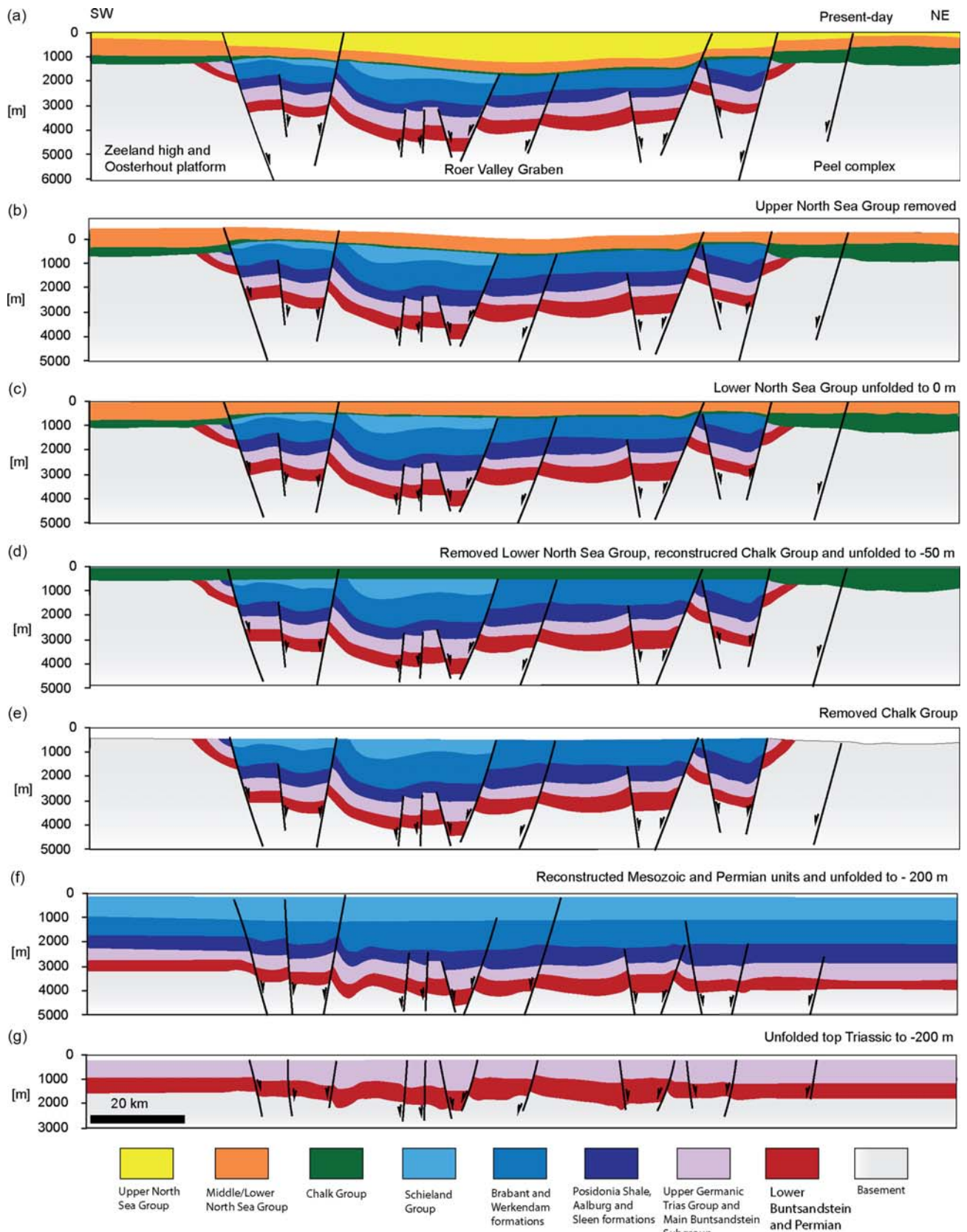
Figure 13. Main steps taken to restore transect EBN018 (see Fig. 4 for the un-interpreted and interpreted seismic line). Some of the interpreted faults in Fig. 4 were removed to simplify the restoration process. Colours refer to specific stratigraphic units (see Fig. 3). Horizon reconstruction is displayed in f) and d).
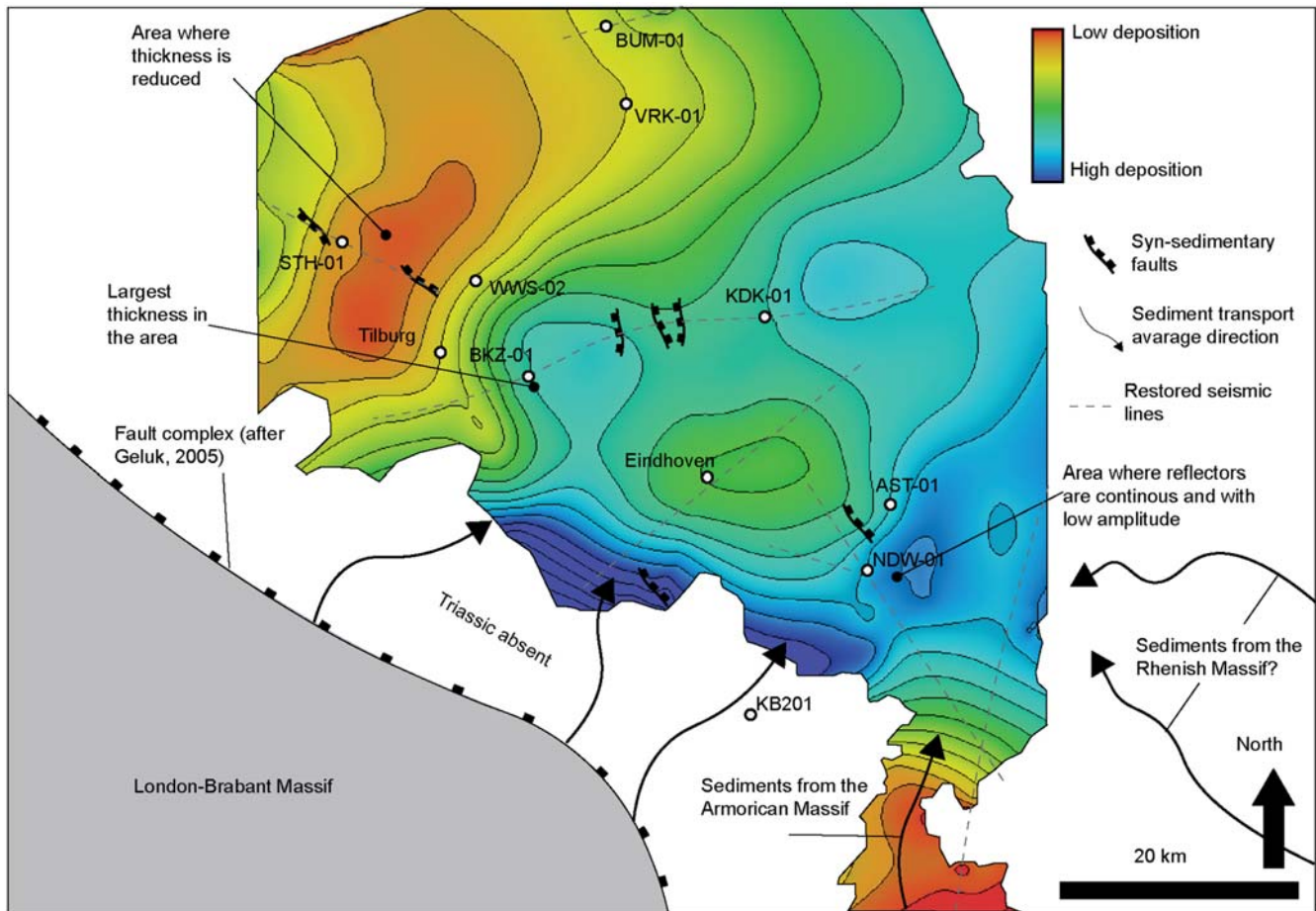
Figure 14. Basin geometry reconstruction derived through merging of the restored seismic transects (displayed as dashed black lines). Colour gives an estimation of the presence of depocenters for the Main Buntsandstein sedimentation. The sedimentation of the Main Buntsandstein Subgroup occurred in a continental setting, with no marine influence.

2005; Geluk, 2007; Palermo et al., 2008; Bourquin et al., 2009). A major river system transported sediments for over 400 km from the Armorican Massif to the north, fed by the substantial precipitation in the remnants of the Variscan orogeny (Mckie and Williams, 2009). The restored base of the Main Buntsandstein and the thickness maps suggest that the area around the Nederweert well (NDW-01) was potentially a locus of deposition for these sediments. During the Early to Middle Triassic times, the Rhenish Massif was also exposed to the southeast of the study area. However, its role as a sediment source during the Main Buntsandstein deposition in the Roer Valley Graben remains unclear (Köppen and Carter, 2000; IF Technology, 2012; Augustsson et al., 2019).

Implications for geothermal exploration

The Main Buntsandstein Subgroup may represent a promising geothermal play in the Roer Valley Graben considering its widespread distribution and expected in situ temperatures between ~60 and ~140°C given the depth ranging from 2 to and 4.5 km and the average geothermal gradient of the area of ~31°C/km (Bonté et al., 2012; Békési et al., 2020). This is in line with borehole temperature measurements across the area, where temperatures of ~120°C are encountered at depths of ~3000 m (IF Technology, 2012).

This study shows that the Main Buntsandstein Subgroup in the Roer Valley Graben is a sand-prone sedimentary succession with sandstone thickness largely above 150 m and N/G on average higher than 50% (Fig. 6c and d). The net sandstone thickness and N/G maps presented in this study are derived from large-scale well interpolation, thus they become more uncertain when moving away from the wells. However, combining these maps with reflector characteristics provides an overview of sandstone distribution across the Roer Valley Graben. A more in-depth study is needed to define these properties locally and to analyse the lithological heterogeneities therein.

The reconstruction of the basin geometry and the sandstone thickness map indicate that the central and the southeast parts of the Roer Valley Graben were active depocenters during the Early Triassic rifting phase, where normal faults create the accommodation space for the deposition of thick sandstone sequences (~150–200 m). In this area, the reflector continuity indicates that these units may be continuous at 4–5 km scale. The lateral continuity of these sandstone units in the southeastern part of the Roer Valley Graben is further supported by their overall low amplitudes, suggesting the occurrence of similar lithologies (Zeng, 2018). Sandbodies are usually well connected in systems with a N/G higher than 30% (Larue and Hovadik, 2006). Although connectivity may be less of an issue in sand-prone reservoirs,

internal sandbody heterogeneities such as permeability barriers and baffles may affect the dynamic behaviour of these types of reservoirs (Mckie, 2011).

In addition, the ~200 m thick Nederweert Sandstone is largely present below the Buntsandstein in the southeastern part of the Roer Valley Graben (IF Technology, 2012). This formation may further enlarge the recovery volume if connected with the Buntsandstein above. However, more research needs to be done to evaluate the distribution and reservoir quality of the Nederweert Sandstone.

IF Technology (2012) suggested that the northern flank of the Roer Valley Graben represents an area where geothermal systems are feasible in the Triassic sediments. Based on the current study, the Buntsandstein has average lower N/G along the northern flank compared to the rest of the Roer Valley Graben. Such a reduction in N/G suggests the connectivity of the sandbodies is more uncertain compared to the southern part of the Roer Valley Graben, where sandstones are thicker and likely better connected. However, the presence of less conductive lithologies such as claystone can produce a thermal blanket effect and increase the temperature of the underlying sandstone units, producing thermal anomalies important to consider when exploring geothermal resources (Hamm and Lopez, 2012).

The Main Buntsandstein in the central part of the Roer Valley Graben has experienced deep burial. With burial, formation water experiences an increase in temperature and pressure that may trigger physical and chemical processes affecting the primary composition and texture of sediments (Milliken, 2003) and, consequently, reservoir properties. The Main Buntsandstein Subgroup sediments experienced burial depths deeper up to ~3–4 km in the central part of the Roer Valley Graben. This is the area where diagenesis may have deteriorated reservoir quality the most making geothermal operations more challenging. This challenge has been exemplified by data from the well NLW-GT-01 in the West Netherlands Basin, which encountered very poor reservoir quality (porosity <5% and permeability <0.1 mD) in the Main Buntsandstein Subgroup at depths of ~4 km as result of diagenesis (Felder and Fernandez, 2018).

The shallower burial depths (~1.5–2.5 km) experienced by the Main Buntsandstein in the platform areas may have instead enhanced the preservation of reservoir quality. Overall, borehole STH-01 shows the best reservoir properties in the basin with an average porosity of ~20% and permeability exceeding 1 Darcy (www.nlog.nl). The well is located on the Oosterhout Platform, where the Main Buntsandstein experienced average shallower maximum burial depths compared to the central parts of the graben, which could have helped in the preservation of the primary porosity. In addition, the Main Buntsandstein sediments were located at surface conditions before the deposition of the Chalk Group, which may have resulted in leaching of the sediments enhancing reservoir properties (Mijnlieff, 2020). This would suggest a higher chance of encountering the best reservoir properties along the southern flank and to the southeast of Eindhoven, where the Triassic is often present at shallow depths below the Chalk Group. However, a more detailed study on diagenesis and its relationship with reservoir properties is needed to confirm this hypothesis.

The Roer Valley Graben is an area affected by faults that largely control the present-day extent of the Main Buntsandstein sediments. Many faults are concentrated along the Roer Valley Graben flanks where the Main Buntsandstein may offer a promising geothermal target due to the shallower burial depths and the higher likelihood to have preserved reservoir quality. Faults create a structural configuration dominated by roughly SE–NW oriented blocks. These faults compartmentalise the Buntsandstein sediments, reducing their extent along the ~SW–NE direction. However, these blocks are continuous over tens of kilometers along the ~SE-NW direction, thus it is likely that a potential doublet could be oriented parallel to the orientation of the faults.

Conclusion

Subsurface mapping integrated with 2D palinspastic restoration of seismic section reveals a heterogeneous nature and distribution of the Main Buntsandstein sediments as a result of an interplay between tectonic activity and depositional processes.

Tectonic activity during the Early to Middle Triassic resulted in depocenter development and a larger thickness of the Main Buntsandstein in the central and southeastern parts of the Roer Valley Graben. After deposition, the Main Buntsandstein sediments were buried down to 3–4 km across the Roer Valley Graben in response to extensional tectonics and the deposition of the Jurassic units above. The Roer Valley Graben flanks were instead subjected to shallower burials and locally the Main Buntsandstein was present at surface conditions during the Middle to Late Jurassic. During Cretaceous times, the Chalk Group was deposited unconformably over an area affected by faulting and tilting. This led to the development of the base Chalk Group unconformity. This unconformity is well visible along the Roer Valley Graben flanks, where the Triassic is often observed to be truncated at the base of the Chalk Group. Subsequently, the Roer Valley Graben was inverted during the Late Cretaceous before subsidence could resume during the Cenozoic, burying the Main Buntsandstein sediments down to maximum burial depths of ~4–4.5 km in the centre of the Roer Valley Graben.

Overall, the present-day architecture of the Main Buntsandstein sediments is largely controlled by faults. Faults create juxtapositions to Carboniferous, Jurassic, and Chalk deposits, and limit the lateral extent of the sediments by post-depositional compartmentalisation of the lower Triassic units.

The largest thicknesses attained in the central and southern parts of the Roer Valley Graben are explained by the presence of fault-induced depocenters during the Early to Middle Triassic. In these areas, sandstone sequence thicknesses are larger, up to 300 m thick, and reflectors exhibit low amplitude and high lateral continuity. To the north, a change in lithology is indicated by the N/G map and stronger amplitude reflectors. Such a change in lithology is also visible upwards in the stratigraphy across the Roer Valley Graben, where an increase in reflector amplitude contrasts seems to reflect a decrease in N/G. The area around STH-01 represented an area where a lower subsidence rate resulted in a reduced thickness of the Main Buntsandstein gross thickness. In terms of extra-basinal sediment sources, the London-Brabant Massif to the southwest, the Armorican Massif to the south and the Rhenish Massif to the east were the major sediment suppliers.

The central part of the Roer Valley Graben appears to be the most promising geothermal target considering the sandstone thicknesses of over 200 m and the lateral reflector continuity over 4–5 km. However, while the deep burial depths may favour high in situ temperatures, the temperatures and pressures experienced at deeper levels may also have enhanced diagenetic processes that deteriorate reservoir properties suggesting the centre of the Roer Valley Graben to be a high-risk target. The adjacent platform areas and the southeastern part of the Roer Valley Graben may instead

represent better targets for further investigation, where shallower burial depths may have helped preserve reservoir quality.

References

Audley-Charles, M.G., 1970. Triassic palaeogeography of the British Isles. Quarterly Journal of the Geological Society **126**(1-4): 49–74.

Augustsson, C., Aehnelt, M., Voigt, T., Kunkel, C., Meyer, M. & Schellhorn, F., 2019. Quartz and zircon decoupling in sandstone: petrography and quartz cathodoluminescence of the Early Triassic continental Buntsandstein Group in Germany. Sedimentology **66**(7): 2874–2893.

Bachmann, G.H., Geluk, M.C., Doornenbal, J.C. & Stevenson, A.G., 2010. Chapter 9, Triassic. *In:* Doornenbal H. & Stevenson A. (eds): Petroleum Geological Atlas of The Southern Permian Basin Area. EAGE Publications B.V. (Houten): 148–173.

Békési, E., Struijk, M., Bonté, D., Veldkamp, H., Limberger, J., Fokker, P.A., Vrijlandt, M. & Van Wees, J.D., 2020. An updated geothermal model of the Dutch subsurface based on inversion of temperature data. Geothermics **88**: 101880.

Bonté, D., Van Wees, J.D. & Verweij, J.M., 2012. Subsurface temperature of the onshore Netherlands: new temperature dataset and modelling. Netherlands Journal of Geosciences **91**(4): 491–515.

Bourquin, S., Guillocheau, F. & Péron, S., 2009. Braided rivers within an arid alluvial plain (example from the Lower Triassic, western German Basin): recognition criteria and expression of stratigraphic cycles. Sedimentology **56**(7): 2235–2264.

Bourquin, S., Bercovici, A., López-Gómez, J., Diez, J.B., Broutin, J., Ronchi, A., Durand, M., Arché, A., Linol, B. & Amour, F., 2011. The Permian-Triassic transition and the onset of Mesozoic sedimentation at the northwestern peri-Tethyan domain scale: palaeogeographic maps and geodynamic implications. Palaeogeography, Palaeoclimatology, Palaeoecology **299**(1-2): 265–280.

Carter, R.R., Cade, C. & Amiri Garoussi, K., 1990. Sedimentology and reservoir quality of the middle and upper Bunter Formations, Cores 1-7 Waalwijk-2. EXT **58541**.

Deckers, J., Rombaut, B., Van Noten, K. & Vanneste, K., 2021. Influence of inherited structural domains and their particular strain distributions on the Roer Valley graben evolution from inversion to extension. Solid Earth **12**(2): 345–361.

Deckers, J., Rombaut, B., Broothaers, M., Dirix, K. & Debacker, T., 2023. New 3D fault model for eastern Flanders (Belgium) providing insights on the major deformation phases in the region since the late Paleozoic. Journal of Structural Geology **166**: 104779.

De Jager, J., 2003. Inverted basins in the Netherlands, similarities and differences. Netherlands Journal of Geosciences **82**(4): 339–349.

Fossen, H., Ksienzyk, A.K., Rotevatn, A., Bauck, M.S. & Wemmer, K., 2021. From widespread faulting to localised rifting: Evidence from K-Ar fault gouge dates from the Norwegian North Sea rift shoulder. Basin Research **33**(3): 1934–1953.

Felder, M. & Fernandez, S., 2018. Core hot shot NLW-GT-01. PanTerra Geoconsultants B.V. (The Hague): 7.

Gawthorpe, R.L. & Leeder, M.R., 2000. Tectono-sedimentary evolution of active extensional basins. Basin Research **12**(3-4): 195–218.

Geluk, M.C., Duin, E.T., Dusar, M., Rijkers, R.H.B., Van den Berg, M.W. & Van Rooijen, P., 1994. Stratigraphy and tectonics of the Roer Valley Graben. Geologie en Mijnbouw **73**: 129–129.

Geluk, M.C. & Röhling, H.G. 1997. High-resolution sequence stratigraphy of the Lower Triassic 'Buntsandstein' In the Netherlands and northwestern Germany. Geologie en Mijnbouw **76**, 227–246.

Geluk, M.C. Stratigraphy and tectonics of Permo-Triassic basins in the Netherlands and surrounding areas (PhD Thesis), 2005, 171, Utrecht University (Utrecht)

Geluk, M., 2007. Triassic. In: Wong Th.E,, Batjes D.A.J. & De Jager J, (eds): Geology of the Netherlands. Royal Netherlands Academy of Arts and Sciences (Amsterdam): 107–125.

Hamm, V. & Lopez, S., 2012. Impact of fluvial sedimentary heterogeneities on heat transfer at a geothermal doublet scale. Stanford Geothermal Workshop, 18 pp.

Herngreen, G.F.W. & Wong, ThE, 2007. Cretaceous. *In:* Wong Th.E., Batjes D.A.J. & De Jager J. (eds): Geology of the Netherlands (Amsterdam, Royal Netherlands Academy of Arts and Sciences, 107–125.

Technology, I.F., 2012. Geothermal energy Noord-Brabant. Geological study of Triassic reservoirs in the province of Noord-Brabant. Summary Report 3/60125/NB.

Köppen, A. & Carter, A., 2000. Constraints on provenance of the central European Triassic using detrital zircon fission track data. Palaeogeography, Palaeoclimatology, Palaeoecology **161**(1-2): 193–204.

Kortekaas, M., Böker, U., Van Der Kooij, C. & Jaarsma, B., 2018. Lower Triassic reservoir development in the northern Dutch offshore. Geological Society, London, Special Publications **469**(1): 149–168.

Kramers, L., Van Wees, J.D., Pluymaekers, M.P.D., Kronimus, A. & Boxem, T., 2012. Direct heat resource assessment and subsurface information systems for geothermal aquifers; the Dutch perspective. Netherlands Journal of Geosciences **91**(4): 637–649.

Kombrink, H., Doornenbal, J.C., Duin, E.J.T., Den Dulk, M., Van Gessel, S.F., Ten Veen, J.H. & Witmans, N., 2012. New insights into the geological structure of the Netherlands; results of a detailed mapping project. Netherlands Journal of Geosciences **91**(4): 419–446.

Larue, D.K. & Hovadik, J.M., 2006. Connectivity of channelized reservoirs: a modelling approach. Petroleum Geoscience **12**: 291–308.

Lingrey, S. & Vidal-Royo, O. Evaluating a 2-D Structural Restoration: Validating Section Balance. *AAPG Annual Convention and Exhibition, Calgary, Alberta, Canada.*

Linol, B., Bercovici, A., Bourquin, S., Diez, J.B., López-Gómez, J., Broutin, J., Durand, M. & Villanueva-Amadoz, U., 2009. Late Permian to Middle Triassic correlations and palaeogeographical reconstructions in south-western European basins: new sedimentological data from Minorca (Balearic Islands, Spain). Sedimentary Geology **220**(1-2): 77–94.

McKie, T. & Williams, B., 2009. Triassic palaeogeography and fluvial dispersal across the northwest European Basins. Geological Journal **44**(6): 711–741.

McKie, T., 2011. Architecture and behavior of dryland fluvial reservoirs, Triassic Skagerrak Formation, central North Sea. *In:* From River To Rock Record: The Preservation Of Fluvial Sediments And Their Subsequent Interpretation SEPM Special Publication No. 97, Copyright. 2011SEPM (Society for Sedimentary Geology), 189–214.

Mijnlieff, H.F., 2020. Introduction to the geothermal play and reservoir geology of the Netherlands. Netherlands Journal of Geosciences **99**: e2.

Milliken, K.L., 2003. Late diagenesis and mass transfer in sandstone shale sequences. *In:* MacKenzie M (ed): Treatise on Geochemistry. vol. **7**, Elsevier (Amsterdam): 159–190.

Ministry of Economic Affairs and Climate Policy (MEA). Directorate-General Energy, Telecommunications and Competition, 2023. Natural resources and geothermal energy in the Netherlands, Annual review. An overview of exploration, production and underground storage. MEA.

Nelskamp, S. & Verweij, J.M. Using basin modelling for geothermal energy exploration in the Netherlands–an example from the West Netherlands Basin and Roer Valley Graben. TNO-060-UT-2012-00245, 113 pp.

NITG, 2004. Geological Atlas of the Subsurface of the Netherlands – onshore. Netherlands Institute of Applied Geoscience TNO (Utrecht): 104 pp.

Olivarius, M., Weibel, R., Friis, H., Boldreel, L.O., Keulen, N. & Thomsen, T.B., 2017. Provenance of the Lower Triassic Bunter Sandstone Formation: implications for distribution and architecture of aeolian vs. **fluvial reservoirs in the North German Basin**. Basin Research **29**: 113–130.

Palermo, D., Aigner, T., Geluk, M., Poeppelreiter, M. & Pipping, K., 2008. Reservoir potential of a lacustrine mixed carbonate/siliciclastic gas reservoir: The Lower Triassic Rogenstein in the Netherlands. Journal of Petroleum Geology **31**(1): 35–96.

Pharaoh, T.C., Dusar, M., Geluk, M., Kockel, F., Krawczyk, C.M., Krzywiec, P., Scheck-Wenderoth, M., Thybo, H., Vejbaek, O. & Van Wees, J.D., 2010. Tectonic evolution. *In:* Petroleum geological atlas of the Southern Permian Basin area, 25–57.

Suppe, J., 1985. Principles of structural geology. Prentice-Hall, Inc., Englewood Cliffs (New Jersey): 537

TNO-GDN. Stratigraphic Nomenclature of the Netherlands, TNO – Geological Survey of the Netherlands 2023. https://www.dinoloket.nl/en/stratigraphic-nomenclature.

Van Adrichem Boogaert, H.A. & Kouwe, W.F.P., 1993-1997. Stratigraphic nomenclature of the Netherlands, revision and update by RGD and NOGEPA. Mededelingen Rijks Geologische Dienst, 50 pp.

Van Lochem, H., Ter Borgh, M. & Mijnlieff, H., 2019. Geological Evaluation for the Seismic Acquisition Programme for SCAN Areas F (Oost-Brabant and Noord-Limburg) and G (Zuid-Limburg). SCAN Programme **2019**: 11.

Veeken, P.P. & Van Moerkerken, B, 2013. Seismic stratigraphy and depositional facies models. EAGE Publications, 496 pp. doi: 10.3997/9789073834439.

Vercouter, C. & Van den Haute, P., 1993. Post-Palaeozoic cooling and uplift of the Brabant massif as revealed by apatite fission-track analysis. Geological Magazine **130**(5): 639–646.

Willems, C.J., Vondrak, A., Mijnlieff, H.F., Donselaar, M.E. & Van Kempen, B.M., 2020. Geology of the Upper Jurassic to Lower Cretaceous geothermal aquifers in the West Netherlands Basin-an overview. Netherlands Journal of Geosciences **99**: e1.

Williams, G.D., Powell, C.M. & Cooper, M.A., 1989. Geometry and kinematics of inversion tectonics. Geological Society, London, Special Publications **44**(1): 3–15.

Winstanley, A.M., 1993. A review of the Triassic play in the Roer Valley Graben, SE onshore Netherlands. Geological Society, London, Petroleum Geology Conference Series **4**(1): 595–607.

Worum, G., Michon, L., van Balen, R.T., Van Wees, J.D., Cloetingh, S. & Pagnier, H., 2005. Pre-Neogene controls on present-day fault activity in the West Netherlands Basin and Roer Valley Rift System (southern Netherlands): role of variations in fault orientation in a uniform low-stress regime. Quaternary Science Reviews **24**(3-4): 473–488.

Zeng, H., 2018. What is seismic sedimentology? A tutorial. Interpretation - A Journal of Bible and Theology **6**(2): 11–12.

Ziegler, P.A., 1992. European Cenozoic rift system. *In:* Ziegler P.A. (ed): Geodynamics of Rifting, Volume I. Case History Studies on Rifts: Europe and Asia. Tectonophysics. vol. **208**, p. 91–111.

Zijerveld, L., Stephenson, R., Cloetingh, S.A.P.L., Duin, E. & Van den Berg, M.W., 1992. Subsidence analysis and modelling of the Roer Valley Graben SE Netherlands. Tectonophysics **208**(1-3): 159–171.